

1 **Pre-print**

2 Bergomi, M. A., Dal Piaz, G. V., Malusà, M. G., Monopoli, B., & Tunesi, A.  
3 (2017)

4 The Grand St Bernard-Briançonnais nappe  
5 system and the Paleozoic inheritance of the  
6 Western Alps unraveled by zircon U-Pb dating  
7 Tectonics, 36(12), 2950-2972.

8 [10.1002/2017TC004621](https://doi.org/10.1002/2017TC004621)

9

10      **The Grand St Bernard - Briançonnais nappe system**  
11      **and the Paleozoic inheritance of the Western Alps**  
12      **unravelled by zircon U-Pb dating**

13  
14      M.A. Bergomi<sup>1</sup>, G.V. Dal Piaz<sup>2</sup>, M.G. Malusa<sup>1\*</sup>, B. Monopoli<sup>3</sup>, A. Tunesi<sup>1</sup>

15

16      <sup>1</sup> Department of Earth and Environmental Sciences, University of Milano-Bicocca, Milano, Italy

17      <sup>2</sup> Department of Geosciences, University of Padova, Padova, Italy

18      <sup>3</sup> LTS - Land Technology & Service, Padova, Italy

19

20      \*Corresponding author: Marco Giovanni Malusa ([marco.malusa@unimib.it](mailto:marco.malusa@unimib.it))

21

22      **Key Points:**

- 23      • First compelling radiometric evidence of Late Devonian orogenic magmatism in the  
24      European Alps
- 25      • Geochronologic record of a complex Ordovician to Permian tectonic evolution along the  
26      northern Gondwana margin
- 27      • Part of the Moldanubian domain was dismembered in the Late Carboniferous and is now  
28      accreted in the Alpine orogenic wedge.
- 29

30    **Abstract**

31    The continental crust involved in the Alpine orogeny was largely shaped by Paleozoic tectono-  
32    metamorphic and igneous events during oblique collision between Gondwana and Laurussia. In  
33    order to shed light on the pre-Alpine basement puzzle disrupted and re-amalgamated during the  
34    Tethyan rifting and the Alpine orogeny, we provide SHRIMP U-Pb zircon and geochemical whole  
35    rock data from selected basement units of the Grand St Bernard – Briançonnais nappe system in the  
36    Western Alps, and from the Penninic and Lower Austroalpine units in the Central Alps. Zircon U-  
37    Pb ages, ranging from  $459.0 \pm 2.3$  Ma to  $279.1 \pm 1.1$  Ma, provide evidence of a complex evolution  
38    along the northern margin of Gondwana including Ordovician transtension, Devonian subduction  
39    and Carboniferous-to-Permian tectonic reorganization. Original zircon U-Pb ages of  $371 \pm 0.9$  Ma  
40    and  $369.3 \pm 1.5$  Ma, from calcalkaline granitoids of the Grand Nomenon and Gneiss del Monte  
41    Canale units, provide the first compelling evidence of Late Devonian orogenic magmatism in the  
42    Alps. We propose that rocks belonging to these units were originally part of the Moldanubian  
43    domain, and were displaced towards the SW by Late Carboniferous strike-slip faulting. The  
44    resulting assemblage of basement units was disrupted by Permian tectonics and by Mesozoic  
45    opening of the Alpine Tethys. Remnants of the Moldanubian domain became either part of the  
46    European paleomargin (Grand Nomenon unit) or part of the Adriatic paleomargin (Gneiss del  
47    Monte Canale unit), to be finally accreted into the Alpine orogenic wedge during the Cenozoic.

48    **Keywords:** Variscan orogeny; microplate amalgamation; magmatism; geochronology; Alps

49    **1. Introduction**

50    The continental crust of stable Europe, from the Ibero-Armorican chain to the Bohemian massif,  
51    is largely shaped by the tectono-metamorphic and igneous events developed from the Ordovician to  
52    the Carboniferous during oblique collision between Gondwana and Laurussia and intervening  
53    Avalonia and Armorica microplates (Ballèvre et al., 2014; Edel et al., 2013; Hatcher, 2002;

54 Martinez Catalan et al., 1990; Neubauer, 2002; Shelley & Bossiere, 2000; Stampfli & Borel, 2002;  
55 von Raumer, 1981, 1998) forming ultimately the Pangea. In the future Alpine domain, the pre-  
56 Variscan and Variscan continental crust was fragmented by the break-up of Pangea starting from  
57 the Permian, and then reworked, accreted and partly rejuvenated by the Meso-Cenozoic Alpine  
58 orogeny (Dal Piaz et al., 2003; Handy et al., 2010; Malusà et al., 2015; Rosenbaum & Lister, 2005;  
59 Schmid et al., 2004). Despite the masking effects of the Alpine overprint, remnants of Permian,  
60 Variscan and older magmatic events are still recognized in some Adria-derived (Austroalpine) and  
61 Europe-derived (Penninic, Helvetic) units (Bonin et al., 1993; Desmons & Mercier, 1993; Thèlin et  
62 al., 1993), providing invaluable insights on the impact of Paleozoic inheritance on Alpine  
63 evolution. This article is mainly focused on the Paleozoic evolution of the Penninic basement units  
64 of the Grand St Bernard - Briançonnais nappe system (Western Alps), and provides new SHRIMP  
65 U-Pb zircon and geochemical whole rock analyses on gneissic bodies derived from acidic intrusive  
66 and subvolcanic protoliths sampled in the Ruitor, Leverogne, Grand Nomenon and Houillère units  
67 exposed in the Aosta Valley (NW Italy). Results are compared with unpublished data from similar  
68 granitoids exposed in the Central Alps, in the Lower-Penninic gneissic nappe of Monte Leone  
69 (Lepontine dome, Steck et al., 2013 and reference therein) and in the Lower-Austroalpine Gneiss  
70 del Monte Canale unit (Bernina nappe s.l., Spillmann & Büchi, 1993). Our new geochemical and  
71 geochronological data are finally discussed within the framework of published U-Pb data from the  
72 broader Alpine region, shedding new light on the Paleozoic inheritance of the Western and Central  
73 Alps, and on the Variscan and pre-Variscan evolution of crustal domains later involved in the  
74 Alpine orogenic belt.

75 **2. Geologic background**

76 The Grand St Bernard - Briançonnais nappe system crops out along the entire arc of the Western  
77 Alps as a first-rank component of the Alpine orogenic wedge ([Figure 1](#)). It includes polycyclic  
78 Variscan and pre-Variscan basement rocks, monocyclic Upper Carboniferous - Lower Triassic

79 siliciclastic successions, Permian igneous bodies and classic Meso-Cenozoic Briançonnais cover  
80 sequences (Bigi et al., 1990; Caby, 1968; Desmons & Mercier, 1993; Ellenberger, 1958; Gouffon,  
81 1993; Sartori et al., 2006; Thelin et al., 1993). These units display a Paleogene  
82 blueschist/greenschist facies metamorphic overprint, and are piled up within a double-vergent  
83 frontal wedge developed during the Alpine orogeny (Beltrando et al., 2010; Bucher & Bousquet,  
84 2007; Malusà et al., 2005a, 2011; Polino et al., 2015). Along the Aosta Valley cross section, the  
85 monocyclic low-grade Houillère unit is exposed in the frontal part of the Paleogene frontal wedge  
86 (De Giusti et al., 2004; Elter, 1987; Polino et al., 2015), and is bounded to the SE by the Internal  
87 Houillère Fault (Malusà et al., 2005b, 2009) ([Figure 2](#)). To the SE of this fault, on the rear part of the  
88 Paleogene frontal wedge, different basement units are stacked along NW-dipping shear zones  
89 chiefly marked by Piedmont zone calcschists (Govi, 1966; Malusà et al., 2005a, Polino et al.,  
90 2015). From the top to the bottom, these units are the Ruitor, Leverogne and Grand Nomenon units  
91 ([Figure 2](#)).

92 The Houillère unit ([Figure 2](#)) consists of low-grade metamorphic rocks derived from Namurian-  
93 Early Stephanian coal-bearing siliciclastic successions, Upper Carboniferous to Lower Triassic  
94 conglomerates and sandstones, and minor Triassic dolostones, evaporites and calcite marbles  
95 (Bertrand et al., 1996; Debelmas et al., 1991; Elter, 1987; Fabre, 1958; Franchi & Stella, 1903;  
96 Polino et al., 2015; Sartori et al., 2006). In the Aosta Valley, it includes the gneissic leucogranite of  
97 Costa Citrin, early interpreted as a Permian laccolith (Caby, 1974), and later dated as Visean-  
98 Namurian (Conventional U-Pb Isotope Dilution: intercept ages at  $324 \pm 17$  Ma and  $323 \pm 8$  Ma;  
99 Bertrand et al., 1998), in contrast with available age constraints in their country rock. On the  
100 southern side of the Aosta Valley, similar rocks are also aligned along the Briançonnais Fault,  
101 which separates the Houillère unit in the hanging wall from the Sion-Courmayeur unit in the  
102 footwall (De Giusti et al., 2004; Elter, 1987; Polino et al., 2015).

103       The Ruitor unit (Caby, 1968; Desmons & Mercier, 1993; Malusà et al., 2005a) ([Figure 2](#)) is part  
104      of the so-called “Briançonnais External zone” together with the Pontis and Siviez-Mischabel  
105      basement units of the Swiss Alps (Burri, 1983; Gouffon, 1993; Sartori et al., 2006; Scheiber et al.,  
106      2014; Steck et al., 2001). Its polycyclic basement consists of metasedimentary sequences, massive-  
107      to-banded amphibolites and deformed Upper Cambrian-Ordovician and Permian intrusive and  
108      subvolcanic rocks (Bertrand et al., 1998, 2000b; Bussy et al., 1996a; Guillot et al., 2002; Scheiber  
109      et al., 2013), and was affected by two main metamorphic events (Baudin, 1987; Caby & Kienast,  
110      1989; Desmons, 1992; Desmons et al., 1999; Detraz & Loubat, 1984; Thélin et al., 1993): an  
111      Alpine event under epidote-blueschist facies conditions (Dal Piaz, 1965; Polino et al., 2015;  
112      Schiavo, 1997) and a pre-Alpine event under amphibolite-facies condition dated at ca. 330 Ma  
113      (Bussy et al., 1996b; Giorgis et al., 1999; Markley et al., 1998). Evidence of an older eclogitic  
114      event is locally preserved in garnet-amphibolites (Schiavo, 1997).

115       The Leverogne and Grand Nomenon units ([Figure 2](#)) exposed farther east are classically referred  
116      to as the Briançonnais Internal zone (Amstutz, 1962; Cigolini, 1995; Dal Piaz & Govi, 1965;  
117      Debelmas et al., 1991; Desmons & Mercier, 1993; Elter, 1987; Polino et al., 2015), together with  
118      the Mont Fort nappe in the nearby Swiss Alps (Sartori et al., 2006; Thélin et al., 1993). These units  
119      show no evidence of the eclogitic relics and Variscan high-grade metamorphic assemblages that are  
120      found in the basement rocks of the Briançonnais External zone (Bertrand et al., 2000b; Cigolini,  
121      1995; Desmons et al., 1999a, 1999b; Guillot et al., 1991, 2012). The Leverogne unit ([Figure 2](#))  
122      consists of garnet-chloritoid micaschist, garnet-glaucophane schists, fine-grained gneisses with  
123      poikilolastic albite, graphite-albite schists, massive quartzites, and abundant mafic and felsic  
124      igneous rocks with pervasive Alpine epidote-blueschist facies metamorphism and greenschist facies  
125      retrogression (Malusà et al., 2005a; Schiavo, 1997). Mafic rocks are garnet-glaucophanites and  
126      greenschists. Felsic rocks were emplaced in the Late Cambrian (Bertrand et al., 2000a, 2000b;  
127      Guillot et al., 1991), and are either referred to as Val di Rhêmes (Bertrand et al., 2000b) or

128 Changier (Polino et al., 2015) metagranophyres. The Grand Nomenon unit ([Figure 2](#)) includes a  
129 major metagranitoid body, corresponding to the Cogne-Valsavarenche pluton or Favret  
130 metagranodiorite of previous work (Amstutz, 1962; Bonin et al., 1993; Dal Piaz, 1928; Novarese,  
131 1909; Polino et al., 2015). The host rock is a fine-grained metasedimentary sequence of garnet-  
132 biotite-chlorite-bearing albitic gneisses, minor quartz-rich schists, quartzites and dark graphitic  
133 phyllites, which are associated to lenses of foliated augengneiss and albite-epidote amphibolite  
134 (Polino et al., 2015). The host rock locally preserves a pre-Alpine epidote-amphibolite facies  
135 foliation, crosscut by metagranitoid body and only partly obliterated by Alpine greenschist-facies  
136 metamorphism (Malusà et al., 2005a). The metagranitoid body, hereafter referred to as Grand  
137 Nomenon pluton for the sake of simplicity, consists of massive to foliated greenschist-facies  
138 derivatives from calcalkaline tonalite and granodiorite, minor quartzdiorite, cumulus gabbro and  
139 aplitic dykes (Cigolini, 1995; Guillot et al., 2012). The intrusion age of the Grand Nomenon pluton  
140 is referred to the earliest Carboniferous based on U-Pb conventional IDTIMS ( $357 \pm 24$  Ma) and  
141 SHRIMP ( $356 \pm 3$  Ma) analyses of igneous zircons (Bertrand et al., 2000a). This age is unique  
142 among the Paleozoic magmatic rocks dated in the axial Western Alps. However, similar rocks are  
143 described in the Central Alps in the Gneiss del Monte Canale unit (Bonsignori et al., 1970; Boriani  
144 et al., 2012a; Nangeroni, 1957; Venzo & Schiavinato, 1970; Venzo et al., 1971;), traditionally  
145 ascribed to the Lower-Austroalpine Bernina nappe s.l. (Spillmann & Büchi, 1993) and exposed in  
146 the “Southern Steep Belt” to the north of the Insubric Fault (Milnes, 1974; Schmid et al., 1987)  
147 ([Figure 1](#)). The Gneiss del Monte Canale unit mainly consists of metagranodiorites with minor  
148 metatonalites, metadiorites and metagranites (hereafter referred to as Monte Canale pluton for the  
149 sake of simplicity), associated with metasediments and mafic rocks metamorphosed under  
150 greenschist facies conditions (Boriani et al., 2012a and references therein). The stable metamorphic  
151 mineral assemblage of these metagranodiorites consists of quartz, K-feldspar, albite, white mica,  
152 pale green amphibole locally with brown core, epidote, chlorite, and minor biotite (Ambiveri et al.,

153 2007). The Monte Canale pluton is cut by coarse- to medium-grained leucogranites without  
154 apparent metamorphic overprint (Ambiveri et al., 2007). The contact with the nearby Upper  
155 Austroalpine units (Languard-Campo nappe, Bergomi & Boriani, 2012; Bianchi et al., 1981;  
156 Notarpietro & Gorla, 1981; Pace, 1966) is marked by a mylonitic belt, and both the Lower and  
157 Upper Austroalpine units are intruded by 310 - 300 Ma old granitoids (Boriani et al., 2012a; von  
158 Riet, 1984), suggesting that they were already juxtaposed at the time of emplacement of the Late  
159 Carboniferous granitoids.

160 Evidence of pre-Variscan magmatism possibly resembling what observed in the Ruitor unit is  
161 instead reported in the Lower Penninic units of the Lepontine dome (Monte Leone nappe; Bergomi  
162 et al., 2007). In the Ossola Valley (NW Italy), the Lepontine nappe stack includes (from the bottom  
163 to the top) the Verampio, Antigorio, Piada di Crana and Monte Leone nappes (Berger et al., 2005;  
164 Bigi et al., 1990; Escher et al., 1993; Grujic & Mancktelow, 1996; Maxelon & Mancktelow, 2005;  
165 Steck et al., 2013), mainly consisting of Upper Carboniferous - Lower Permian granitoids (305-290  
166 Ma, Bergomi et al., 2007) with minor metapelites, marbles and amphibolite lenses. The Monte  
167 Leone nappe includes fine-grained banded orthogneisses and minor coarse-grained augengneiss  
168 interlayered with paragneisses, hornblende gneisses and amphibolites, and shows a penetrative  
169 amphibolite-facies metamorphic overprint of Alpine age that is common to other nappes of the  
170 Lepontine dome (Maxelon & Mancktelow, 2005, and references therein).

171 **3. Sampling strategy and methods**

172 Analyzed samples are metagranitoids and orthogneisses from the main tectonic units of the  
173 Grand St-Bernard nappe exposed in the Aosta valley. Dated samples ([Figure 1 and 2](#)) are two  
174 orthogneisses of the Ruitor unit (samples s1 and s2), the Changier metagranophyre of the  
175 Leverogne unit (sample s3), the metagranitoid of the Grand Nomenon pluton (sample s4), and the  
176 Costa Citrin metaleucogranite of the Houillère unit (sample s5). We have also analyzed some  
177 gneissic granitoids from the Monte Leone Nappe in the Lepontine dome (sample s6) and from the

178 Gneiss del Monte Canale unit in the Bernina nappe (sample s7) for comparison ([Figure 1](#)).  
179 Geochemical analyses of samples s1 to s7 were integrated by analysis of additional samples (see  
180 the full list of samples in the supporting information, [Table TS02](#)).

181 All samples were analyzed for major, minor and trace elements (results are listed in [Table](#)  
182 [TS02](#)). They are very fresh, with LOI (Loss On Ignition) in agreement with the modal  
183 abundance of hydrous phases. Samples selected for SHRIMP U-Pb dating (s1 to s7) are  
184 representative of granitoids occurring in each area ([Figure 1](#)) and the results are reported in  
185 [Table TS01](#). We base our discussion on the Concordia ages calculated after Ludwig (1998) in a  
186 Tera-Wasserburg Concordia diagram (Tera & Wasserburg, 1972). Errors given for Concordia  
187 ages in the text are reported at  $2\sigma$  level. A more detailed discussion of the methodology can be  
188 found in the supporting information (see also Black et al., 2003; Compston et al., 1992;  
189 Ludwig, 2003a; 2003b; Nasdala et al., 2008; Schöne et al., 2006; Stacey & Kramers, 1975;  
190 Steiger & Jäger, 1977; Williams, 1998).

191 **4. Results**

192 SHRIMP U-Pb and whole rock geochemical analyses are listed in [Table TS01](#) and [TS02](#),  
193 respectively. They are shown in [Figures 3, 4 and 5](#), and described in full below. Sample locations,  
194 petrography and ages are summarized in [Table TS03](#).

195 **4.1 Zircon U-Pb geochronology**

196 Grand St Bernard - Ruitor unit (samples s1 and s2). Zircons from samples s1 (Basse Tête  
197 augengneiss) and s2 (Les Lacerandes augengneiss, Thèlin et al., 1993) share similar size, shape and  
198 internal CL texture. They are transparent, colorless, prismatic and euhedral in shape. They show a  
199 variable size (150-300  $\mu\text{m}$  long) with an aspect ratio (width-to-length) from 1:2 to 1:3. Some of  
200 them contain small apatite inclusions. In CL imaging ([Figure 3h-s1, s2](#)), they present inherited  
201 cores mantled by magmatic overgrowths showing a faint and concentric zoning (Corfu et al., 2003

202 and references therein). U (145-707 ppm) and Th (15-96 ppm) contents, as well as Th/U (0.1-0.5)  
203 ratios confirm their magmatic origin ([Table TS01](#); Hoskin & Schaltegger, 2003 and references  
204 therein). Inherited cores from both samples mainly span over a small time interval of concordant  
205 and nearly concordant ages from  $829.3 \pm 10.6$  to  $567.8 \pm 4.1$  Ma ([Table TS01](#)), which can be  
206 roughly grouped into clusters of Cryogenian ( $687 \pm 18.5$  to  $829.3 \pm 10.6$  Ma) and Ediacaran ( $567.8$   
207  $\pm 4.1$  to  $605.3 \pm 8.8$  Ma) ages. Only one inherited core yielded a Paleoproterozoic age of  $2016.2 \pm$   
208 71.8 Ma ([Table TS01](#)). SHRIMP U-Pb analyses performed on magmatic overgrowths turned out  
209 Concordia ages of  $459.0 \pm 2.3$  Ma (n = number of analyses = 14; MSWD = Mean Square of  
210 Weighted Deviates = 0.2; Prob. = Probability of fit = 1.0) and  $456.4 \pm 2.4$  Ma (n = 15; MSWD =  
211 0.1; Prob. = 1.0) for samples s1 and s2, respectively ([Figure 3a and b](#)). We interpret these Late  
212 Ordovician ages as the time of crystallization of the granitic protholiths. Guillot et al. (2002)  
213 reported Ordovician emplacement ages (IDTIMS and SIMS U-Pb analyses on zircon; upper  
214 intercepts at  $460 \pm 7$ ,  $468 \pm 22$ ,  $469 \pm 15$  and  $471 \pm 5$  Ma) for other orthogneiss protholiths  
215 occurring in the Ruitor basement on the southern side of the Aosta Valley.

216 Grand St Bernard - Leverogne unit (sample s3). Zircons from sample s3 are pale pink,  
217 transparent, prismatic and euhedral in shape and rich of inclusions. They are 150-200 up to 300  $\mu\text{m}$   
218 in length, with an aspect ratio of 1:2. Highly metamict grains are abundant in the selected zircon  
219 population. In CL images, metamict zircons have dark cores surrounded by highly luminescent and  
220 structureless rims. Few SHRIMP U-Pb analyses (e.g., spots 1.1, 2.1 and 6.1, [Table TS01](#)) carried  
221 out on these rims produced discordant and meaningless ages probably due to the presence of a high  
222 proportion of common lead ([Table TS01](#)). Zircons without metamict alteration show thin and faint  
223 concentric and oscillatory zoning ([Figure 3h-s3](#)), with typical U (122-762 ppm), Th (25-202 ppm)  
224 and Th/U (0.1-1) magmatic values ([Table TS01](#)). Eighteen SHRIMP U-Pb analyses performed on  
225 core and rims produced a Middle Ordovician Concordia age of  $465.0 \pm 2.5$  Ma (MSWD = 0.3;

226 Prob. = 1.0; [Figure 3c](#)), which can be regarded as the emplacement age of the metagranophyre  
227 protholith. Only one inherited core Ediacaran in age has been observed.

228 Grand St Bernard - Grand Nomenon unit (sample s4). Zircons from sample s4 are pale pink in  
229 color and transparent to cloudy. They are mainly euhedral and prismatic in shape, although a few  
230 have irregular faces with smoothed edges. They are predominantly 100 – 200 µm in length, with an  
231 aspect ratio of 1:2-2.5. Apatite is the main inclusion. Fracturing is often associated with brownish  
232 metamict areas. They present a fine magmatic growth zonation ([Figure 3h-s4](#)) and sector zoning  
233 defined by patches of relative CL brightness. CL textures along with high U (632-1827 ppm) and  
234 Th (177-897 ppm) contents and Th/U (0.3-0.5) ratios ([Table TS01](#)) suggest an igneous origin for  
235 these zircon grains. SHRIMP U-Pb analyses performed both on cores and rims provided a Late  
236 Devonian Concordia age of  $371 \pm 0.9$  Ma (n = 17; MSWD = 0.5; Prob. = 1.0; [Figure 3d](#)), which  
237 represents the emplacement age of the protholith. Only one Ediacaran inherited core was measured  
238 ([Table TS01](#)).

239 Grand St Bernard - Houillère unit (sample s5). Zircons from sample s5 are pink, transparent and  
240 euhedral needle-like crystals up to 250-300 µm long, with an aspect ratio of 1:2. They are rich in  
241 inclusions. Some stubby and highly metamict zircons are present. In CL imaging, they have typical  
242 magmatic concentric and oscillatory zoning ([Figure 3h-s5](#)). CL textures, U (77-2150 ppm) and Th  
243 (90-1261 ppm) contents, as well as Th/U (0.2-0.5) ratios ([Table TS01](#)) suggest a magmatic origin  
244 for these zircon grains. SHRIMP U-Pb analyses both on cores and rims yielded an Early Permian  
245 Concordia age of  $279.1 \pm 1.1$  Ma (n = 14; MSWD = 0.4; Prob. = 1.0; [Figure 3e](#)), which is our best  
246 estimate as emplacement age of the protholith. One spot analysis performed on stubby and highly  
247 metamict zircon produced an apparent older and discordant age of  $334.0 \pm 3.8$  Ma probably due to  
248 a high proportion of common lead (spot 8.1; [Table TS01](#)). Bertrand et al. (1998) reported two  
249 poorly constrained upper intercept ages at  $324 \pm 24$  and  $323 \pm 7$  Ma (IDTIMS U-Pb on zircon) for  
250 two metagranites occurring in the Houillère unit at the Costa Citrin locality.

251 Lepontine dome - Monte Leone (sample s6). A nearly undeformed sample was selected for  
252 SHRIMP geochronology. Zircons in sample s6 are colorless and transparent with apatite as main  
253 inclusions. They are mainly euhedral and prismatic in shape, predominantly 100 – 200 µm in  
254 length, with an aspect ratio of 1:1.5. In CL images, zircon grains present typical magmatic  
255 concentric and oscillatory growth from core to rim ([Figure 3h-s6](#)). Some zircon grains show instead  
256 inherited cores surrounded by magmatic overgrowths. The ages of inherited cores range from 563 ±  
257 8 to 962 ± 10 Ma ([Table TS01](#)). Thirteen spot analyses performed both on well-defined concentric  
258 and oscillatory zoning and on magmatic overgrowths gave a concordant age of 457.9 ± 3.5 Ma  
259 ([Figure 3f](#)). According to zircon textures and U-Th geochemistry (U=137-590 ppm, Th=24-214  
260 ppm, Th/U=0.1-0.4), this age could be interpreted as the emplacement age of the protolith of the  
261 Ordovician metagranitoids.

262 Lower Austroalpine – Gneiss del Monte Canale unit (sample s7). Zircons from sample s7 are  
263 pale pink to colorless and transparent to cloudy, with apatite as main inclusion. Zircons are mostly  
264 euhedral and prismatic in shape, 150 – 200 µm in length, and with an aspect ratio of about 1:2. In  
265 CL images ([Figure 3h-s7](#)), zircon texture is mainly characterized by concentric and oscillatory  
266 zoning, which suggests along with U (547-1968 ppm), Th (161-856 ppm) and Th/U (0.2-0.5)  
267 values an igneous origin ([Table TS01](#)). Only few grains have inherited cores. Fifteen SHRIMP spot  
268 analyses performed both on cores and rims provided a Late Devonian Concordia age of 369.3 ± 1.5  
269 Ma (n = 15; MSWD = 0.3; Prob. = 1.0; [Figure 3g](#)), which represents the emplacement age of the  
270 granitoid. This age is similar within error to the emplacement age obtained from the Grand  
271 Nomenon sample.

## 272 **4.2 Geochemistry**

273 Grand St Bernard - Ruitor unit. The Upper Ordovician granitoids collected in the Ruitor unit are  
274 metaluminous to peraluminous granites [A/CNK = molar  $\text{Al}_2\text{O}_3/(\text{CaO}+\text{Na}_2\text{O}+\text{K}_2\text{O})$  = 1.06 – 1.18]  
275 ([Figure 4a and b](#)), and lie in the high-K calcalkaline field of the  $\text{K}_2\text{O}$  vs  $\text{SiO}_2$  diagram ([Figure 4c](#);

276 Peccerillo & Taylor, 1976). According to the classification proposed by Frost et al. (2001), they are  
277 magnesian metagranites ([Figure 4d](#)) straddling the boundary between the calc-alkalic and alkali-  
278 calcic fields ([Figure 4e](#)). On the primitive mantle (PM) normalized multi-element variation diagram  
279 ([Figure 5a](#)), they show typical calcalkaline patterns with enrichment in LILE (Large Ion Lithophile  
280 Elements) over HFSE (High Field Strength Elements), troughs at Sr-P, Nb and Ti and peaks at Th,  
281 K and Pb. They are also enriched in LREE (Light Rare Earth Elements) with respect to HREE  
282 (Heavy Rare Earth Elements) ([Figure 5b](#)), and they show  $(\text{La/Yb})_N = 12.23 - 13.01$  and negative  
283 Eu anomalies ( $\text{Eu/Eu}^* = 0.59 - 0.62$ ).

284 Grand St Bernard - Leverogne unit. The Middle Ordovician granophyres of the Leverogne unit  
285 are mainly metaluminous ( $A/\text{CNK} = 0.98 - 1.03$ ) alkali granites with silica content of 75.2 – 75.6  
286 wt% ([Figure 4a and b](#)). They have high  $K_2O$  content ([Figure 4c](#)), are ferroan granitoids and plot in  
287 the alkali-calcic field ([Figure 4d and e](#)).  $\text{FeO}^{\text{tot}}/\text{MgO}$  ratios vary from 4.8 to 11.1 with an average of  
288 7.3 that is higher than values observed in I-type, S-type and M-type granites (Whalen et al., 1987).  
289 They are also characterized by high  $\text{Ga}/\text{Al}$  ratios ( $10,000 \times \text{Ga}/\text{Al} > 2.6$ ) and high  $\text{Zr}+\text{Nb}+\text{Ce}+\text{Y}$   
290 concentrations (446 - 467 ppm), suggesting an A-type geochemical character (Whalen et al., 1987).  
291 On the PM-normalized multi-element variation diagram ([Figure 5c](#)), they are characterized by  
292 negative Ba, Nb, P, Zr and Ti, and positive Rb, Th-U and K anomalies. The samples are enriched in  
293 LREE relative to HREE ([Figure 5d](#)), with positive LREE slope [ $(\text{La/Sm})_N = 2.84 - 3.11$ ], relatively  
294 flat HREE [ $(\text{Gd/Yb})_N = 1.16 - 1.26$ ] and a pronounced Eu anomaly ( $\text{Eu/Eu}^* = 0.17 - 0.21$ ).

295 Grand St Bernard - Grand Nomenon unit. The Upper Devonian granitoids from the Grand  
296 Nomenon pluton are metaluminous ( $A/\text{CNK} = 0.75 - 0.91$ ) diorites and granodiorites ([Figure 4a](#)  
297 [and b](#)) showing high-K calcalkaline affinity ([Figure 4c](#)). They plot as magnesian calc-alkalic  
298 granitoids ([Figure 4d and e](#)). On PM normalized multi-element variation diagram ([Figure 5e](#)), they  
299 are enriched in LILE with respect to HFSE with troughs at Rb-Ba, Nb-Ta, P and Ti, and peaks at K,

300 Pb and Nd-Zr. They present LREE enrichment over HREE ([Figure 5f](#)), with  $(\text{La/Yb})_{\text{N}} = 7.36 -$   
301 20.67 and slight negative Eu anomalies ( $\text{Eu/Eu}^* = 0.77 - 0.79$ ).

302 The most evolved sample ( $\text{SiO}_2 > 75 \text{ wt\%}$ ) is a peraluminous ( $\text{A/CNK} = 1.16$ ) and high-K  
303 calcalkaline leucogranite ([Figure 4a, b and c](#)) plotting in the ferroan and calc-alkalic field ([Figure](#)  
304 [4d and e](#)).

305 Grand St Bernard - Houillère unit. The Costa Citrin gneissic body of the Houillère unit derives  
306 from a metaluminous ( $\text{A/CNK} = 0.99$ ) Lower Permian granite ([Figure 4a and b](#)), with high silica  
307 ( $\text{SiO}_2 = 73.81 \text{ wt\%}$ ) and total alkali ( $\text{Na}_2\text{O} + \text{K}_2\text{O} = 9.09$ ) contents and high  $\text{FeO}^{\text{tot}}/\text{Mg} (= 5.9)$  and  
308  $\text{K}_2\text{O}/\text{Na}_2\text{O} (= 1.23)$  ratios. It plots close to the boundary between high-K calcalkaline and  
309 shoshonitic series in the  $\text{K}_2\text{O}$  vs.  $\text{SiO}_2$  diagram ([Figure 4c](#)). Although its agpaitic index of 0.90  
310 supports its A-type geochemical feature, this sample is not strictly A-type but more likely  
311 transitional. In fact, it does not satisfy an A-type chemical signature in terms of trace elements, such  
312 as low  $10,000^*\text{Ga/Al} (< 2.6)$  ratio and  $\text{Zr} + \text{Nb} + \text{Ce} + \text{Y}$  content (Whalen et al., 1987). The PM  
313 normalized pattern shows LILE enrichment over HFSE, with troughs at Ba, Nb, P, Zr and Ti, and  
314 peaks at U, K and Pb ([Figure 5g](#)). The REE pattern is enriched in LREE relative HREE ([Figure 5h](#)),  
315 with  $(\text{La/Sm})_{\text{N}} = 4.43$ , flat HREE pattern [ $(\text{Gd/Yb})_{\text{N}} = 1.16$ ] and negative Eu anomaly ( $\text{Eu/Eu}^* =$   
316 0.31).

317 Lepontine dome - Monte Leone. The Upper Ordovician Monte Leone granitoids are mainly  
318 granitic in composition and generally metaluminous to peraluminous, with  $\text{A/CNK}$  ratio close to 1  
319 (0.9-1.2) and  $\text{A/NK}$  ratio between 1 and 2 ([Figure 4a and b](#)). All samples follow a typical  
320 calcalkaline trend and plot in the high-K calcalkaline field ([Figure 4c](#)). On the PM-normalized  
321 diagram, they are enriched in LILE (Cs, Rb, Ba, Th, U, K) with respect to HFSE and show marked  
322 negative P, Ba, Nb and positive Pb and Zr spikes ([Figure 5a](#)). Their REE pattern is characterized by  
323 LREE enrichment (100 – 300 times) compared to HREE (6-20 times;  $(\text{La/Yb})_{\text{N}} = 5.5 - 12.6$ ) and by  
324 a negative Eu anomaly ( $\text{Eu/Eu}^* = 0.46-0.72$ ) ([Figure 5b](#)).

325 Lower Austroalpine – Gneiss del Monte Canale unit. The Upper Devonian samples from the  
326 Monte Canale pluton are dioritic to granitic in composition with high-K calc-alkaline affinity and a  
327 metaluminous character ( $A/CNK = 0.85-1.09$ ) ([Figure 4a, b and c](#)). They plot as magnesian  
328 granitoids straddling the alkali-calcic and calc-alkalic boundary ([Figure 4d and e](#)). On the PM-  
329 normalized multi-element variation diagram ([Figure 5e](#)), they are enriched in LILE over HFSE,  
330 with peaks at Pb and Zr and troughs at Ba, Nb and Ti. Their REE pattern is characterized by  
331 enrichment in LREE (40-130 times) over HREE (6-25 times), a slightly positive Eu anomaly  
332 ( $Eu/Eu^* = 0.90 - 0.98$ ) and  $(La/Yb)_N = 8-11$  ([Figure 5f](#)). The leucogranites present high-silica  
333 content ( $SiO_2 > 75$  wt%), peraluminous character ( $A/CNK > 1.2$ ) but scattered  $K_2O$  content ([Figure](#)  
334 [4b and c](#)). They are mainly magnesian granites straddling calc-alkalic and alkali-calcic fields in  
335 [Figure 4d and e](#).

336 **5. Discussion**

337 Age, paleogeographic significance and tectonic evolution of orthogneisses in the pre-Mesozoic  
338 basements across southern Europe and the Alps have long been the subject of interest and  
339 controversies. The Paleozoic inheritance of the basement units exposed in the Central and Western  
340 Alps is supported by groups of modern isotope dating, which are interpreted as a mark of magmatic  
341 and metamorphic events occurring before and after the unconformable deposition of Upper  
342 Carboniferous coal-bearing sedimentary rocks atop the Variscan orogenic belt (Dal Piaz, 1939).  
343 Evidence of Late Proterozoic to Cambrian and even older events is provided by U-Pb ages on  
344 zircons from metasediments (Gauthiez et al., 2011; Manzotti et al., 2015, 2016) and igneous bodies  
345 from various basement units of the Alpine belt (Bussien et al., 2011; Neubauer, 2002; Poller, 1997,  
346 Schaltegger et al., 1997; Scheiber et al., 2014; Schulz et al., 2008). At that time, these units were  
347 probably assembled to the Gondwana margin, to be later tectonically dismembered and re-  
348 amalgamated since the Devonian during the Variscan orogeny (Stampfli & Borel, 2002; von  
349 Raumer et al., 2013). Unfortunately, geochemical and geochronologic datasets about Variscan and

350 pre-Variscan protholiths in the Central and Western Alps are largely incomplete, and most  
351 geochronologic ages are referred to low-retentivity isotopic systems.

352 **5.1. Ordovician magmatic cycle**

353 Upper Cambrian-Ordovician magmatic rocks are distributed from Iberia to the Bohemian Massif  
354 through the Pyrénées and the French Massif Central (Ballèvre et al., 2014; Castiñeira et al., 2008;  
355 Friedl et al., 2004; Melletton et al., 2010; Sanchez-García et al., 2003). Current geodynamic  
356 reconstructions generally agree about the occurrence of a Cambrian to Early Ordovician active  
357 continental margin all along northern Gondwana, associated to the southward subduction of the  
358 Iapetus Ocean (Kroner & Romer, 2013; von Raumer & Stampfli, 2008). By contrast, the  
359 interpretation of post-Early Ordovician magmatism is problematic, and several models have been  
360 proposed so far for the post-Cambrian evolution of the northern Gondwana margin (e.g., Kroner &  
361 Romer, 2013; von Raumer et al., 2013).

362 In the Alpine domains, Ordovician granitoids and coeval basic rocks cover a time span ranging  
363 from 480 Ma to 420 Ma (Neubauer, 2002; Schaltegger & Gebauer, 1999; von Raumer et al., 2002).  
364 According to data presented in this work, high-K metaluminous to peraluminous calcalkaline  
365 granites were emplaced during the Late Ordovician in the Ruitor unit ( $459.0 \pm 2.3$  and  $456.4 \pm 2.4$   
366 Ma) and in the Monte Leone basement ( $457.9 \pm 3.5$  Ma) ([Figure 3a, b and f](#)). In the Grand St  
367 Bernard - Briançonnais nappe system ([Figure 6](#)), other geochemically similar granitic protholiths  
368 ([Figure 5a and b](#)) are documented in the Ruitor ( $468 \pm 22$ ,  $465 \pm 11$ ,  $460 \pm 7$  Ma, Guillot et al.,  
369 2002), Siviez-Mischabel (~460 Ma, Genier et al., 2008), Sapey (Modane metagranites:  $452 \pm 5$  Ma;  
370 Bertrand et al., 2000a) and Ligurian Briançonnais (470 – 455 Ma, Gaggero et al., 2004) basement  
371 units. Metagranitoids with similar age ([Figure 6](#)) and geochemistry ([Figure 5a and b](#)) are also  
372 preserved in the Dora-Maira unit ( $457 \pm 2$  Ma, Bussy & Cadoppi, 1996), the Lower Penninic units  
373 of the Central Alps (Gruff Complex:  $453 \pm 8.4$  Ma, Galli et al., 2011; Adula Nappe: Garenstock  
374 augengneiss 446 - 460 Ma and Rossa orthogneiss 455 - 460 Ma, Caravagna-Sani et al., 2014;  $457 \pm$

375 4 Ma, Liati et al., 2009; Sambuco nappe:  $464.3 \pm 8$  Ma, Bussien et al., 2011), the Eastern  
376 Austroalpine nappes (Languard-Campo:  $448 \pm 14$  Ma, Boriani et al., 2012a; Silvretta: “Younger  
377 Orthogneiss”  $451 \pm 2$  Ma, Flisch, 1987), and the Southern Alps (Serie dei Laghi: 450 - 460 Ma,  
378 Pezzotta & Pinarelli, 1994; Fioraro Complex:  $462 \pm 11$  Ma, Bergomi et al., 2004).

379 The geochemical features of these rocks (high LILE/HFSE, LREE/HFSE and Th/Yb ratios, low  
380 Nb content, negative Nb and positive Pb spikes; [Figure 5a and b](#)) could be consistent with those of  
381 modern continental and island arc granitoids (e.g., Tatsumi & Eggins, 1995), and may be  
382 interpreted as the arc to backarc evolution of a convergent plate margin (Schaltegger et al., 1997;  
383 Stampfli et al., 2011). However, their geochemical calcalkaline signature may not necessarily imply  
384 a direct linkage with a coeval supra-subduction setting, but may result from a range of shallow  
385 processes such as mixing of distinct magma batches, fractional crystallization and interaction with  
386 crustal components. Granites with calcalkaline geochemical signatures are observed, for instance,  
387 in transtensional-extensional settings characterized by a heterogeneously metasomatized sub-  
388 continental mantle, such as the Cenozoic Basin and Range Province in the US (Hawkesworth et al.,  
389 1995) and the Permian igneous province in Europe (Dal Piaz, 1993; Dal Piaz & Martin, 1998;  
390 Marotta & Spalla, 2007; Schaltegger & Brack, 2007). Plutonic rocks of intermediate composition  
391 generally dominate modern active continental margins (Wilson, 1989), whereas continental rift  
392 zones often show a geochemically bimodal magmatism, with calcalkaline granites and alkali  
393 granites (granophyres) associated to minor basic rocks and layered gabbro-peridotite batholiths  
394 (Costa & Rey, 1995; Wilson et al, 2004). In the latter case, many different magma types, possibly  
395 including I-type and S-type granites as well as alkaline to tholeiitic basalts, are expected after  
396 melting of lower crust and mantle sources (Finger & Steyrer, 1995; Floyd et al., 2000).

397 In the Grand St Bernard - Briançonnais basements, the pre-Variscan magmatic cycle generally  
398 starts with ~500 Ma old granophyres and granites (Scheiber et al., 2014). These rocks are  
399 sometimes ascribed to the continental rifting that preceded the opening of the Rheic Ocean along

400 the northern Gondwana margin (von Raumer et al., 2013), as possibly confirmed by the occurrence  
401 of a ~496 Ma old plagiogranite in the Chamrousse ophiolite (Helvetic Belledonne massif, Ménot et  
402 al., 1988). Metagranophyres from the Levorogne unit (sample s3) share a ferroan and  
403 metaluminous geochemical behavior with the Val di Rhêmes – Changier granophyre ([Figure 5c](#) and  
404 [d](#)) dated at  $511 \pm 9$  Ma by Bertrand et al. (2000b). However, our sample s3 yielded a much younger  
405 emplacement age of  $465.0 \pm 2.5$  Ma ([Figure 3c](#)). Ages of ~500 Ma were instead obtained in  
406 metamict zircon grains from sample s3, but they were discarded due to their high proportion of  
407 common Pb ([Table TS01](#)). As a result, the Leverogne metagranophyres fall in the same time  
408 interval (470 - 450 Ma) of both calcalkaline granites and volumetrically minor basic rocks  
409 described in the Briançonnais basement. The Middle to Upper Ordovician protoliths of these  
410 Briançonnais orthogneisses are generally intruded within pelitic and arenaceous successions of Late  
411 Neoproterozoic to Cambrian age, as indicated by inherited zircon cores in our analyzed samples  
412 ([Table TS01](#)). They are closely associated with boudins of mafic rocks (eclogites) and massive to  
413 banded amphibolite sills (Thèlin et al., 1993). The eclogitic protoliths recognized in the Ruitor and  
414 Siviez-Mischabel basements are not dated yet, but protolith ages of  $468 \pm 22$  and  $471 \pm 5$  Ma were  
415 determined for banded amphibolites of the Ruitor unit (Guillot et al., 2002). Similar ages were also  
416 found in gabbroic sills of the Mont Fort basement that are emplaced within a coeval volcanic-  
417 detrital succession (456.7 - 460 Ma; Gauthiez et al., 2011), and in mafic rocks from the Ligurian  
418 Briançonnais ( $469 \pm 6$  Ma, Gaggero et al., 2004; Giacomini et al., 2007), the Helvetic External  
419 Massifs ( $463 +3/-2$  and  $458 \pm 5$  Ma, Bussy et al., 2011;  $467 +5/-4$  and  $471 +6/-7$  Ma, Oberli et al.,  
420 1994;  $453 +3/-2$  Ma, Paquette et al., 1989;  $462 \pm 6$  Ma, Rubatto et al., 2001;  $478 \pm 5$  Ma,  
421 Schaltegger et al., 2003) and the Eastern Austroalpine Silvretta nappe ( $467 \pm 14$  Ma, Poller, 1997).

422 The occurrence of such bimodal magmatism in a relatively short time interval (470-450 Ma) is  
423 supportive of magma emplacement within a transtensional to extensional setting along the northern  
424 Gondwana margin, which is also in line with the high-T metamorphic event at 450-420 Ma

425 reported in the Eastern Austroalpine and Helvetic domains (Rode et al., 2012; Schulz et al., 2008;  
426 Thöny et al., 2008; von Raumer et al., 2013). These bimodal magmatic features are common to all  
427 of the pre-Variscan basement units of the Central and Western Alps, which may suggest that all of  
428 these units were possibly part of the same thinned-continental-crust domain in northern Gondwana  
429 during Middle to Late Ordovician times.

430 **5.2. Devonian magmatic cycle**

431 The Variscan belt is generally envisaged as a collage of terranes (Matte et al., 1990; Stampfli &  
432 Borel, 2002) variously assembled from the Late Devonian to the Early Permian along the southern  
433 margin of Laurussia (including the Avalonia microcontinent), with generation and exhumation of  
434 granulites and eclogites, partial melting and formation of anatetic migmatites, emplacement of  
435 granitoids and development of sedimentary basins. A number of plutons intruded the Variscan belt  
436 in a time window of ~80 Ma ([Figure 7a](#)). An early pre-collisional pulse of medium to high-K  
437 calcalkaline melts developed in the Late Devonian to Early Carboniferous (380 - 345 Ma). It was  
438 followed by syn-orogenic high-K calcalkaline to shoshonitic magmatism at 345 - 330 Ma, and then  
439 by the intrusion of post-collision magmas at 330 - 300 Ma, associated with penetrative low-pressure  
440 and high-temperature regional metamorphism and anatetic migmatites (e.g., Žák et al., 2014).  
441 Evidence of this evolution is partly preserved in the Grand St Bernard nappe (Grand Nomenon  
442 pluton) and in the Lower-Austroalpine Bernina nappe (Monte Canale pluton). Our analyses of the  
443 Grand Nomenon pluton provided a Late Devonian age of  $371 \pm 0.9$  Ma ([Figure 3d](#)), interpreted as  
444 the age of the protholith, which is slightly older than the age previously reported by Bertrand et al.  
445 (2000b) (upper intercepts at  $363 \pm 24$  and  $353 \pm 3$  Ma). In our samples, data spots between 350 and  
446 360 Ma were discarded because of suspect Pb loss ([Table TS01](#)). A quite similar Late Devonian  
447 emplacement age of  $369.3 \pm 1.5$  Ma was determined for the metagranodioritic protholith of the  
448 Monte Canale pluton ([Figure 3g](#)). Therefore, the Grand Nomenon and the Monte Canale plutons  
449 not only share a similar lithology (mainly metagranodiorites with minor metadiorites and

450 metagranites) and geochemical trends ([Figure 4](#) and [5e-f](#), high-K magnesian calcalkaline  
451 granitoids), but also the same emplacement age ([Figure 3d and g](#)). The less evolved samples ( $\text{SiO}_2$   
452 < 60%, [Figure 5e and f inset](#)), where the effects of fractional crystallization and crust contamination  
453 are not expected to mask the primary features of the magma source, show deep troughs in HFSE on  
454 PM-normalized diagrams coupled with strong enrichment of hydrous-fluid mobile LILE, resulting  
455 in high LILE/HFSE (e.g.,  $\text{Ba}/\text{Nb} > 27.4$ ), LREE/HFSE ( $\text{La}/\text{Nb} > 1.8$ ) and  $\text{Th}/\text{Yb} (> 7.65)$  ratios,  
456 which are typical of a supra-subduction setting (Tatsumi & Eggins, 1995; Wilson, 1989). This is  
457 also suggested by the quite primitive radiogenic isotopic signature of the Grand Nomenon  
458 metadiorites ( $\text{Nd}_{360}$  from -1.2 to +0.9,  $^{87}\text{Sr}/^{86}\text{Sr}_{360}$  from 0.7054 to 0.7063, Guillot et al., 2012).

459 The Grand Nomenon and Monte Canale plutons may have Alpine counterparts in the  $374 \pm 10$   
460 Ma old high-K calcalkaline metagranodiorite from the Penninic basement of the Tauern window  
461 (Zwölferkogel gneiss, Eichhorn et al., 2000), in the Devonian-Carboniferous Rennfeld metatonalite  
462 suite and trondhjemite from the easternmost Austroalpine (Neubauer et al., 2003) and in the  
463 Helvetic domain where a Devono-Dinantian age is cited by Guillot & Ménot (2009) ([Figure 7a](#)). In  
464 the stable European basement north of the Alps, coeval and geochemically comparable granitoids  
465 ([Figure 5e and f](#)) are exposed in the Bohemian Massif (380–370 Ma, Kosler et al., 1995; Venera et  
466 al., 2000; Žák et al., 2011), in the northern French Massif Central (380-350 Ma, Faure et al., 2005;  
467 Pin & Paquette, 2002) and in the southern Armorican domain (373 +6/-11 Ma, Faure et al., 2005,  
468 and references therein) ([Figure 7a](#)).

469 A number of ~340 Ma old syn-collisional shoshonitic granites were dated in Corsica (e.g., Rossi  
470 et al., 2009) and in the External Crystalline Massifs (Guillot & Ménot, 2009), whereas post-  
471 collisional granites were emplaced at ~340 Ma in the Eastern Alps (Eichhorn et al., 2000) and at  
472 320-315 Ma in the Helvetic domain (Guillot & Ménot, 2009; Rubatto et al., 2001), Sardinia and  
473 Corsica (Rossi et al., 2009) ([Figure 7a](#)). The Monte Canale pluton, metamorphosed under  
474 greenschist facies condition, is cut by a coarse-grained peraluminous leucogranite ([Figure 4](#); Monte

475 Canale samples with  $\text{SiO}_2 > 75$  wt%) intruded at ~320 Ma (von Quadt et al., 1994). The Late  
476 Devonian emplacement of the Monte Canale pluton pre-dates the Variscan collision, whereas the  
477 crosscutting unmetamorphosed leucogranites were emplaced in a post-collisional setting. Both  
478 magmatic suites were later intruded by Upper Carboniferous high-K calcalkaline tonalites to  
479 granites (310-300 Ma; Boriani et al., 2012a; von Riet, 1984). The Grand Nomenon granitoids are  
480 similarly intruded by coarse-grained peraluminous leucogranites, which might be coeval with those  
481 crosscutting the Monte Canale pluton ([Figure 4](#); Grand Nomenon sample with  $\text{SiO}_2 > 75$  wt%), but  
482 no Late Carboniferous igneous ages are reported from the Grand St Bernard igneous bodies.

483 Even though the Gneiss del Monte Canale and the Grand Nomenon units may partly share their  
484 magmatic evolution with the Helvetic External Massifs (Guillot & Ménot, 2009; Rubatto et al.,  
485 2001) and the Eastern Alps (Eichhorn et al., 2000), many uncertainties arise about their linkage  
486 with potential counterparts in stable Europe. According to von Raumer et al. (2013), the Late  
487 Devonian-Early Carboniferous arc-related magmatism would be the result of the southward  
488 subduction of the Rheic Ocean beneath a composite peri-Gondwana terrane. Guillot and Ménot  
489 (2009) proposed an extensional back arc setting for the Late Devonian to Dinantian magmatism in  
490 the Helvetic domain, possibly associated to the southeastward subduction of the Saxo-Thuringian  
491 Ocean. Rossi et al. (2009) suggested for the Silurian–Devonian magmatism of Corsica-Sardinia a  
492 northward oceanic subduction beneath Armorica, possibly followed by oblique continental collision  
493 between Armorica and Gondwana during the Late Devonian-Early Carboniferous. Neubauer and  
494 Handler (1999) proposed a northward subduction of a pre-Carboniferous oceanic basin beneath the  
495 southern margin of the Moldanubian domain, in order to explain the Late Devonian-Early  
496 Carboniferous magmatism in the Eastern Alps. Discriminating among the above tectonic models is  
497 beyond the aims of this study. However, the Variscan orogeny was also characterized by relevant  
498 orogen-parallel tectonic displacements as attested by the occurrence of major strike-slip shear zones  
499 (Carosi et al., 2012; Edel et al., 2013; Eichhorn et al., 2000; Guillot & Ménot, 2009; Hatcher, 2002;

500 Martinez Catalan et al., 1990; Shelley & Bossiere, 2000; von Raumer, 1998). The present-day  
501 relative position of the Grand Nomenon and Monte Canale plutons compared to their potential  
502 counterparts in stable Europe may thus reflect a complex geodynamic scenario involving terrane  
503 dispersion by well-documented dextral shear zones active along the boundary of the Moldanubian  
504 domain ([Figure 7b](#)), followed by Early Permian transtension, Mesozoic rifting and Alpine nappe  
505 stacking.

506 **5.3. Permian magmatic cycle**

507 The Late Carboniferous to Early Mesozoic was a period of general plate reorganization, marking  
508 the evolution from compressional to extensional tectonics. In the Western Alps, Early Permian  
509 emplacement of mafic melts at depth (Dal Piaz, 1993; Manzotti et al, 2017; Marotta & Spalla,  
510 2007, and references therein) was associated with (and followed by) bimodal volcanism and  
511 intrusion of granites and pegmatites in the upper crust (Dal Piaz & Martin, 1998; Dallagiovanna et  
512 al., 2009; Schaltegger & Brack, 2007; Schaltegger & Gebauer, 1999).

513 The Houillère unit includes the Lower Permian ( $279.1 \pm 1.1$  Ma, [Figure 3e](#)) Costa Citrin  
514 leucogranite, which shows high-K transitional affinity. Coeval and geochemically similar  
515 granitoids ([Figures 5g, h and 6](#)) and volcanics crop out both in the Briançonnais External zone  
516 (Randa augengneiss:  $269 \pm 2$  Ma, Bussy et al., 1996b; Le Bautsé orthogneiss:  $290 \pm 4$  and  $272 \pm 4$ ,  
517 Scheiber et al., 2014) and in the Briançonnais Internal zone (Mont Fort nappe, Goli d'Aget ignimbritic  
518 metarhyolite: 267 - 280 Ma, Derron et al., 2006; Laget metaignimbrite: 267 - 282 Ma, Bussy et al.,  
519 1996b) of the Grand St Bernard – Briançonnais nappe system ([Figure 6](#)). Permian magmatic zircon  
520 cores are reported from metamorphic granite bodies ( $267 \pm 1$  and  $272 \pm 2$  Ma) in the Valaisan units  
521 atop the Penninic Frontal Thrust (Versoyen zone; Beltrando et al., 2007). Discordant intrusions of  
522 porphyritic granite within Variscan high-grade paragneisses and migmatites are dated as Lower  
523 Permian in the eclogitized continental crust units of Monte Rosa ( $270 \pm 4$  and  $268 \pm 4$  Ma, Pawlig  
524 & Baumgartner, 2001;  $272 \pm 4$  Ma, Liati et al., 2001), Gran Paradiso ( $269 \pm 6$  and  $277 \pm 4$  Ma,

525 Bertrand et al., 2000a;  $277 \pm 4$  and  $272 \pm 3$  Ma, Bertrand et al., 2005;  $269 \pm 6.5$  and  $270.2 \pm 5$  Ma,  
526 Ring et al., 2005) and Dora-Maira (275 - 276, Gebauer et al., 1997;  $290 \pm 2$ ,  $288 \pm 2$  and 283 - 267  
527 Ma, Bussy & Cadoppi, 1996) ([Figure 6](#)). Similar intrusion ages are also reported, for the  
528 Austroalpine units of the Western Alps, in the metagranites and augengneisses of the Dent Blanche  
529 (Arolla series:  $289 \pm 2$  Ma, Bussy et al., 1998), Mt Emilius ( $293 \pm 3$  Ma, Bussy et al., 1998) and  
530 Sesia-Lanzo (Mucrone:  $286 \pm 2$  Ma, Paquette et al., 1989) ([Figure 6](#)). The age of volcanic rocks in  
531 the Briançonnais units of the Ligurian Alps ranges from  $286 \pm 3$  to  $273 \pm 2$  Ma (Dallagiovanna et  
532 al., 2009). In the Central Alps, basement units with Briançonnais affinity s.l. include gneissic  
533 granitoids derived from Permian protoliths (Roffna Complex in Suretta nappe: 290-265 Ma,  
534 Marquer et al., 1998; Scheiber et al., 2013; Truzzo granite in Tambò nappe:  $268 \pm 0.8$  Ma, Marquer  
535 et al., 1998) ([Figure 6](#)). Early Permian acidic igneous products are also widespread in the western-  
536 central Southern Alps (e.g., Gretter et al., 2013; Pinarelli et al., 1988; Schaltegger & Brack, 1999,  
537 2007) ([Figure 6](#)). There is general consensus in connecting the Early Permian calc-alkaline  
538 magmatism in the Alps with the incoming lithospheric thinning and strike-slip tectonics that was  
539 followed, after the Mid-Permian magmatic gap, by regional extension and K-rich volcanics in the  
540 Late Permian (Dallagiovanna et al., 2009; Schaltegger & Brack, 2007). Moreover, the Late  
541 Variscan collapse seems to have developed diachronously, with ages getting progressively younger  
542 from the internal to the external zones of the Variscan belt (Dallagiovanna et al., 2009 and  
543 reference therein). The oldest igneous bodies are dated at 310–296 Ma in the Helvetic External  
544 Massifs (Bussy et al., 2000; Guerrot & Debon, 2000), 320–280 Ma in Sardinia (Oggiano et al.,  
545 2007), 307–300 Ma in Corsica (Cocherie et al., 1994; Paquette et al., 2003; Rossi et al., 2009;  
546 Tommasini et al., 1995), 310–290 Ma in the Lepontine dome (Bergomi et al., 2007; Bussien et al.,  
547 2011) and 310-300 Ma in the Bernina nappe (Boriani et al., 2012; von Riet, 1984). Relatively  
548 younger bodies ( $\leq 290$  Ma; e.g., Schaltegger & Brack, 2007) occur instead in the Adria-derived  
549 Dent Blanche-Sesia basements (293-286 and 285-260 Ma, respectively) and in the Southern Alps

550 (Figure 6). In this regard, the occurrence of Late Variscan igneous bodies in the Bernina nappe  
551 (310-300 Ma, Boriani et al., 2012a) could be supportive of a more internal position of these rocks  
552 within the Variscan belt. On the other hand, the absence of Upper Carboniferous magmatic  
553 products and the occurrence of Lower Permian intrusives and volcanics may point to a more  
554 external position for the External Briançonnais units, i.e., closer to the Gondwana foreland. The  
555 similarity of Lower Permian magmatic products in the Briançonnais, Austroalpine and Southalpine  
556 domains, both in terms of geochemical affinity (Figure 5g and h) and intrusion age (Figure 6), are  
557 consistent with the classic palinspastic reconstructions of the westernmost segment of the future  
558 Alpine region before the onset of Tethyan rifting, and consequent development of the European and  
559 Adriatic passive margins later involved in the Alpine orogeny (e.g., Beltrando et al., 2014; Malusà  
560 et al., 2016).

561 **5.4. Paleogeographic implications**

562 Based on the geochemical and geochronological data presented here, along with literature data  
563 on the Western and Central Alps with particular regard to the basement units of the Helvetic  
564 External Massifs and the Southern Alps that poorly suffered or escaped at all the Alpine  
565 metamorphism, we can speculate as follows:

566 (1) The pre-Variscan features of the studied basement units mimic those of other Alpine  
567 domains (e.g., Southern Alps, Pinarelli & Boriani, 2007) with Late Neoproterozoic and/or  
568 Cambrian pelitic-arenaceous successions intruded by basic and acidic igneous rocks within the  
569 framework of a Middle to Late Ordovician transtensional to extensional geodynamic setting.  
570 Because this pre-Variscan scenario is common to many other Gondwana-derived Alpine domains,  
571 we can consider that the pre-Variscan Briançonnais basements were all part of the thinned  
572 Gondwana margin.

573 (2) The Briançonnais and Bernina basement units preserve evidence of the Late Devonian to  
574 Carboniferous Variscan evolution. In the Ruitor, and other polycyclic basements of the

575 Briançonnais External zone, the Variscan orogeny is only documented by metamorphic fabrics and  
576 polyphase mineral assemblages. Metasediments and associated bodies of gneissic granitoids display  
577 relicts of an amphibolite facies metamorphism dated at ~330 Ma, whereas mafic rocks also  
578 preserve, in places, evidence of an early high-pressure event not dated yet in the External  
579 Briançonnais. This Variscan metamorphic evolution is common to other basement units of the Alps  
580 (e.g., Southern Alps, Pinarelli & Boriani, 2007), in which a main amphibolite facies metamorphism  
581 is locally preceded by a high-pressure event dated at ~400 Ma in Sardinia, ~392-376 Ma in the  
582 Ligurian Briançonnais (Giacomini et al., 2007), ~340 Ma in the Helvetic Argentera massif (Rubatto  
583 et al., 2010), ~340 and ~380 Ma in the Adula nappe of the Lepontine dome (Liati et al., 2009),  
584 ~351 Ma in the Silvretta nappe (Ladenhauf et al., 2001) and 340 – 360 Ma in the Eastern  
585 Austroalpine (Melcher & Meisel, 2004; Miller & Thöni, 1995; Thöni, 2003; Tumiati et al., 2003).  
586 By contrast, basement rocks of the Briançonnais Internal zone escaped both high-pressure and  
587 high-temperature Variscan metamorphism, but they were intruded (Grand Nomenon unit), along  
588 with the Bernina nappe (Gneiss del Monte Canale unit), by Upper Devonian arc-related plutons  
589 metamorphosed under greenschist facies conditions, and then crosscut by a ~320 Ma old  
590 peraluminous leucogranite. The Late Devonian magmatism highlights a close relationship of these  
591 basement units with the Bohemian Massif, the southern Armorican Massif and the northern French  
592 Massifs Central ([Figure 7a](#)). In this view, the polycyclic units of the Briançonnais Internal zone and  
593 the Bernina nappe were probably part of the Moldanubian domain ([Figure 7b](#)) and were possibly  
594 displaced towards the SW by dextral strike-slip faulting in the Late Carboniferous (Carosi et al.,  
595 2012; Edel et al., 2013; Guillot & Ménot, 2009; Matte, 2001; Muttoni et al., 2003) ([Figure 7b](#)),  
596 probably between 320 and 300 Ma as already proposed by Giacomini et al. (2007) and Rolland et  
597 al. (2009).

598 (3) From the Late Carboniferous to the Early Permian, the future Alpine domain was  
599 characterized by a change of geodynamic regime, from Variscan collision to post-Variscan

600 transtension and lithospheric extension propagating across a collage of terranes of different age and  
601 tectono-thermal history (Dallagiovanna et al., 2009; Manzotti et al., 2014; Marotta & Spalla, 2007;  
602 Schuster & Stüwe, 2008; Spalla et al., 2014; von Raumer et al., 2013). The Variscan orogenic belt  
603 was dismembered by dextral shear zones, in turn probably connected to the incoming Palaeo-  
604 Tethys subduction beneath Eurasia. Strike-slip faulting and lithospheric extension were associated  
605 to the emplacement of post-collisional igneous bodies from crustal and subcrustal sources, as well  
606 as to the opening and infilling of intramontane basins in the Houillère zone and, later on, in the  
607 Helvetic and westernmost Southalpine domains. The common occurrence of Lower Permian  
608 magmatic rocks ([Figure 6](#)) in the Houillère and Internal Briançonnais units, in the Southalpine  
609 basement and in the Austroalpine units of Dent Blanche and Sesia-Lanzo suggest that all of these  
610 units were already amalgamated before the opening of the Alpine Tethys. Despite the Variscan  
611 inheritance was of primary importance in shaping the European and Adriatic continental margins  
612 (Guillot et al., 2009; Malusà et al., 2015; 2016), the remnants of the Moldanubian domain  
613 represented by the Grand Nomenon and Gneiss del Monte Canale units became part of opposite  
614 continental margins facing the Alpine Tethys ([Figure 7b](#)), and are now accreted in the Alpine  
615 orogenic wedge either as part of the Europe-derived Grand St Bernard nappe (Grand Nomenon  
616 unit) or as part of the Adria-derived Austroalpine nappes (Gneiss del Monte Canale unit).

617

## 618 **6. Conclusions**

619 New SHRIMP U-Pb zircon and geochemical whole rock analyses carried out on gneissic  
620 igneous bodies of the Grand St Bernard - Briançonnais nappe system of the Western Alps and  
621 surrounding units, shed new light on the Paleozoic evolution of the Variscan and pre-Variscan  
622 continental crust involved in the Alpine orogeny, leading to the following main conclusions:

- 623 1) The Grand St Bernard - Briançonnais nappe system preserves the evidence of a complex  
624 tectonic evolution at the northern margin of Gondwana, starting from transtension in the

Ordovician, followed by subduction in the Devonian and final terrane amalgamation before the onset of Alpine orogeny.

- 2) Basement units of the Briançonnais Internal zone (Grand Nomenon unit) and Bernina nappe (Gneiss del Monte Canale unit) were intruded by high-K calc-alkaline granitoids in the Late Devonian. Geochronological analyses on the Grand Nomenon and Monte Canale plutons provide the first compelling evidence of Late Devonian magmatism in the Alps.
  - 3) The Briançonnais Internal zone and the Bernina nappe were possibly part of the Moldanubian domain, and were displaced towards the SW by strike-slip faulting in the Late Carboniferous ([Figure 7b](#)).
  - 4) The resulting Late Carboniferous assemblage of Variscan and pre-Variscan basement units was dismembered by strike-slip tectonics during the Permian and by the opening of the Alpine Tethys during the Mesozoic. At that time, remnants of the Moldanubian domain now exposed in the Alps became part either of the European (Grand Nomenon unit) or of the Adriatic (Gneiss del Monte Canale unit) paleomargin ([Figure 7b](#)), to be finally accreted in the Alpine orogenic wedge during the Cenozoic.

### **Acknowledgments and data**

Work funded by Fondo di Ateneo of Milano-Bicocca University and by Regione autonoma Valle d'Aosta (Progetto CARG). The manuscript benefited from insightful comments by F. Neubauer, B. Petri and G. Manatschal. All data for this study are presented in the manuscript and in the supporting information, or may be acquired through sources cited. This paper is dedicated to the memory of Marco Beltrando, who enthusiastically focused his brilliant research to the analysis of the complex geologic puzzle of the Western Alps from Alpine subduction back to the Tethyan rifting stages, and to the memory of Alessio Schiavo, who mapped the Grand St Bernard basement providing petrological estimates on the metamorphic evolution of the Ruitor unit.

649

## 650 REFERENCES

- 651 Ambiveri, C., Bergomi, M. A., Boriani, A., & Tunesi, A. (2007). Variscan greenschist facies metamorphism in  
652 the central Alps: the Monte Canale Unit (Bernina Nappe-Lower Austroalpine), *Geoitalia, Epitome*, 2, 161.
- 653 Amstutz, A. (1962). Notice pour une carte géologique de la vallée de Cogne et de quelques autres espaces au  
654 sud d'Aoste. *Archives Sci. Genève*, 15(1), 1-104.
- 655 Ballèvre, M., Martínez Catalán, J. R., López-Carmona, A., Pitra, P., Abati, J., Díez Fernández, R., Ducassou,  
656 Arenas, R., Bosse, V., Castiñeiras, P., Fernández-Suárez, J., Gómez Barreiro, J., Paquette, J. L.,  
657 Peucat, J. J., Poujol, M., Ruffet, G., & Sánchez Martínez, M. (2014). Correlation of the nappe stack in  
658 the Ibero-Armorican arc across the Bay of Biscay: a joint French-Spanish Project. In K. Schulmann, J.  
659 R. Martínez Catalán, J. M. Lardeaux, V. Janousek, G. Oggiano (Eds.), *The Variscan orogeny: extent,  
660 timescale and the formation of the European crust.* (Vol. 405, pp. 77–113). London, UK: Geological  
661 Society of London.
- 662 Bakos, F., Del Moro, A., & Visonà, D. (1990). The Hercynian volcano-plutonic association of Ganna (Lake  
663 Lugano, Central Southern Alps, Italy). *Eur. J. Mineral.*, 2, 373–383.
- 664 Baudin, T. (1987). *Etude géologique du Massif du Ruitor (Alpes franco-italiennes): évolution structurale d'un  
665 socle briançonnais.* (PhD thesis). Grenoble, F: Univ. of Grenoble.
- 666 Beltrando, M., Rubatto, D., Compagnoni, R., & Lister, G. S. (2007). Was the Valaisan basin floored by  
667 oceanic crust? Evidence of Permian magmatism in the Versoyen Unit (Valaisan Domain, Western  
668 Alps). *Ophioliti*, 32, 85–99.
- 669 Beltrando, M., Rubatto, D., & Manatschal, G. (2010). From passive margins to orogens: The link between  
670 Ocean-Continent Transition zones and (Ultra-)High-Pressure metamorphism. *Geology*, 38, 559–562.
- 671 Beltrando, M., Manatschal, G., Mohn, G., Dal Piaz, G. V., Brovarone, A. V., & Masini, E. (2014).  
672 Recognizing remnants of magma-poor rifted margins in high-pressure orogenic belts: The Alpine case  
673 study. *Earth Sci. Rev.*, 131, 88–115.
- 674 Berger, A., Mercolli, I., & Engi, M. (2005). The central Leontine Alps: Notes accompanying the tectonic  
675 and petrographic map sheet Sopra Ceneri (1:100 000). *Schweiz. Miner. Petrogr.*, 85, 109–146.
- 676 Bergomi, M.A., & Boriani, A. (2012). Late Neoproterozoic - Early Paleozoic accretion of the Southalpine  
677 and Austroalpine basements of Central Alps (Italy). *Géol. Fr.*, 1, 69.
- 678 Bergomi, M. A., Colombo, A., Tunesi, A., Caironi, V., & Boriani, A. (2004). *Ordovician granitoids in the  
679 Southern Alps basement (Monte Fioraro Complex-Central Alps): geochemistry and SHRIMP U-Pb  
680 zircon age.* Paper presented at 32nd IGC conference, Firenze, IT. Abstract volume, 2, 1062.
- 681 Bergomi, M.A., Tunesi, A., Shi Y, J. R., Colombo A., & Liu, D. Y. (2007). *SHRIMP II U/Pb  
682 geochronological constraints of pre-Alpine magmatism in the Lower Penninic Units of the Ossola  
683 Valley (Western Alps, Italy).* Paper presented at EGU2007 conference, Vienna, AT. Geophysical  
684 Research Abstr., 9, 07780.
- 685 Bertrand, J. M., & Leterrier, J. (1997). Granitoides d'âge Paléozoïque inférieur dans le socle de Vanoise  
686 méridionale : géochronologie U-Pb du métagranite de l'Arpont (Alpes de Savoie, France). *Comptes  
687 Rendus de l'Académie des Sciences (Paris)*, série II, 325, 839-844.
- 688 Bertrand, J. M., Ailleres, L., Gasquet, D., & Macaudiere, J. (1996). The Pennine Front zone in Savoie  
689 (Western Alps), a review and new interpretation from the Zone Houillère Briançonnaise. *Eclogae Geol.  
690 Helv.*, 89, 297-320.
- 691 Bertrand, J. M., Guillot, F., Leterrier, J., Perruchot, M. P., Ailleres, L. & Macaudiere, J. (1998). Granitoides  
692 de la zone houillère briançonnaise (Alpes occidentales): géologie et géochronologie U-Pb. *Geodin.  
693 Acta*, 11, 33-49.

- 694 Bertrand, J. M., Pidgeon, R. T., Leterrier, J., Guillot, F., Gasquet, D., & Gattiglio, M. (2000a). SHRIMP and  
695 IDTIMS U-Pb zircon ages of the pre-Alpine basement in the Internal Western Alps (Savoy and  
696 Piemont). *Schweiz. Miner. Petrogr.*, 80, 225-248.
- 697 Bertrand, J. M., Guillot, F., & Leterrier, J. (2000b). Age paléozoïque inférieur (U-Pb sur zircon) de  
698 métagranophyres de la nappe du Grand-Saint-Bernard (zona interna, vallée d'Aoste, Italie). *C.R. Acad.  
699 Sci. Paris*, D 330, 473-478.
- 700 Bertrand, J. M., Paquette, J. L., & Guillot, F. (2005). Permian zircon U-Pb ages in the Gran Paradiso massif:  
701 revisiting post-Variscan events in the Western Alps. *Schweiz. Miner Petrogr.*, 85, 19-29.
- 702 Beucler, M., Guillot, F., & Hernandez, J. (2000). Les granophyres du Mont Pourri (Vanoise septentrionale-  
703 Savoie): lithostratigraphie et pétrologie. *Bull. Soc. Vaudoise Sci. Nat.*, 87, 29-60.
- 704 Bianchi-Potenza, B., Gorla, L., & Notarpietro, A. (1978). La "Formazione di Valle Crosina": revisione dei  
705 suoi aspetti petrografici in un nuovo contesto geologico. II-Gli "gneiss minimi". *Rend. Soc. Miner.  
706 Petrol.*, 34, 371-385.
- 707 Bigi, G., Castellarin, A., Coli, M., Dal Piaz, G. V., Sartori, R., Scandone, P., & Vai, G. B. (1990). Structural  
708 Model of Italy scale 1:500.000, sheet 1. SELCA Firenze, I: C.N.R., Progetto Finalizzato Geodinamica.
- 709 Black L.P., Kamo, S. L., Allen, C. M., Aleinikoff, J. N., Davis, D. W., Korsch, R. J., & Foudoulis, C.  
710 (2003). Temora 1: a new zircon standard for Phanerozoic U-Pb geochronology. *Chem. Geol.*, 200, 155-  
711 170.
- 712 Bonin, B., Brändlein, P., Bussy, F., Desmons, J., Eggenberger, U., Finger, F., Graf, K., Marro, C., Mercalli,  
713 I., Oberhänsli, R., Ploquin, A., von Quadt, A., von Raumer, J., Schaltegger, U., Steyrer, H. P., Visonà,  
714 D., & Vivier, G. (1993). Late Variscan magmatic evolution of the Alpine basement. In J. von Raumer,  
715 F. Neubauer (Eds.), *Pre-Mesozoic Geology in the Alps*. (pp. 171-201). Heidelberg, D: Springer-Verlag.
- 716 Bonsignori, G., Bravi, C. E., Nangeroni, G., & Ragni, U. (1970). La geologia del territorio della provincia di  
717 Sondrio. Sondrio, I: Amministrazione Provinciale.
- 718 Boriani, A., Bergomi, M. A., Ferrario, A., & Migliacci Bellante, R. (2012a). Basamento metamorfico  
719 austroalpino, in Autori Vari, Note Illustrative della Carta Geologica d'Italia alla scala 1:50.000, Foglio  
720 056 Sondrio, pp. 49-69, ISPRA.
- 721 Boriani, A., Bergomi, M. A., & Ferrario, A. (2012b). Basamento metamorfico delle Api Meridionali (con  
722 metapluoniti ordoviciane), in Autori vari, Note Illustrative della Carta Geologica d'Italia alla scala  
723 1:50.000, Foglio 056 Sondrio, pp. 69-84, ISPRA.
- 724 Bucher, K., & Bousquet, S. (2007). Metamorphic evolution of the Briançonnais units along the ECORS-  
725 CROP profile (Western Alps): new data on metasedimentary rocks. *Swiss J. Geosci.*, 100, 227-242.
- 726 Burri, M. (1983). Le front du Grand St-Bernard du val d'Herens au val d'Aoste. *Eclogae Geol. Helv.*, 76(3),  
727 469-490.
- 728 Bussien, D., Bussy, F., Magna, T., & Masson, H. (2011). Timing of Palaeozoic magmatism in the Maggia  
729 and Sambuco nappes and paleogeographic implications (Central Lepontine Alps). *Swiss J. Geosci.*, 104,  
730 1-29.
- 731 Bussy, F., & Cadoppi P. (1996). U-Pb zircon dating of granitoids from the Dora-Maira massif (western  
732 Italian Alps). *Schweiz. Miner. Petrogr.*, 76, 217-233.
- 733 Bussy, F., & von Raumer, J. (1994). U-Pb geochronology of Palaeozoic magmatic events in the Mont-Blanc  
734 Crystalline Massif, Western Alps. *Schweiz. Miner. Petrogr.*, 74, 514-515.
- 735 Bussy, F., Derron, M. H., Jacquod, J., Sartori, M., & Thélin, P. (1996a). The 500 Ma-old Thyon meta-  
736 granit: a new A-type granite occurrence in the western Penninic Alps (Valais, Switzerland). *Eur. J.  
737 Mineral.*, 8, 565-575.
- 738 Bussy, F., Sartori, M., & Thélin, P. (1996b). U-Pb zircon dating in the middle Penninic basement of the  
739 Western Alps (Valais, Switzerland). *Schweiz. Miner. Petrogr.*, 76, 81-84.

- 740 Bussy, F., Venturini, G., Hunziker, J. C., & Martinotti, G. (1998). U-Pb ages of magmatic rocks of the western  
741 Austroalpine Dent-Blanche-Sesia Unit. *Schweiz. Miner. Petrogr.*, 78, 163-168.
- 742 Bussy, F., Hernandez, J., & von Raumer, J. (2000). Bimodal magmatism as a consequence of the post-  
743 collisional readjustement of the thickened Variscan continental lithosphere (Aiguilles Rouges-Mont  
744 Blanc massifs, Western Alps). *Trans. Royal Soc. Edinburgh, Earth Sciences*, 91, 221–233.
- 745 Bussy, F., Péronnet, V., Ulianov, A., Epard, J. L., & von J. Raumer, J. (2011). Ordovician magmatism in the  
746 external French Alps: witness of a peri-Gondwanan active continental margin. In J. C. Gutiérrez-Marco,  
747 I. Rábano, D. García-Bellido (Eds.), *Ordovician of the World*, (Vol. 14, pp. 75-82). Madrid, E:  
748 Cuadernos del Museo Geominero, Instituto Geológico y Minero de España.
- 749 Caby, R. (1968). Contribution à l'étude structurale des Alpes occidentales; subdivisions stratigraphiques et  
750 structure de la zone du Grand-Saint-Bernard dans la partie sud du Val d'Aoste (Italie). *Géol. Alpine*, 44,  
751 95-111.
- 752 Caby, R. (1974). Gneiss permo-carbonifères d'origine magmatique et volcanique dans la zone houillère et la  
753 zone du Grand-Saint-Bernard en Val d'Aoste (Italie). *Géol. Alpine*, 50, 39-44.
- 754 Caby, R., & Kienast, R. (1989). Meso-Alpine high-pressure assemblages and excavation of the Ruitor  
755 Briançonnais basement (Savoie, Val d'Aoste, Graie Alps). *Terra Abstracts*, 1, 266.
- 756 Caravagna Sani, M., Epard, J. L., Bussy, F., & Ulianov, A. (2014). Basement lithostratigraphy of the Adula  
757 nappe: implications for Palaeozoic evolution and Alpine kinematics. *Int. J. Earth Sci.*, 103, 61-82.
- 758 Carosi R., Montomoli, C., Tiepolo, M., & Frassi, C. (2012). Geochronological constraints on post-collisional  
759 shear zones in the Variscides of Sardinia (Italy). *Terra Nova*, 24, 42-51.
- 760 Castiñeiras, P., Navidad, M., Liesa, M., Carreras, J., & Casas, J. M. (2008) U-Pb zircon ages (SHRIMP) for  
761 Cadomian and Early Ordovician magmatism in the Eastern Pyrenees: New insights into the pre-  
762 Variscan evolution of the northern Gondwana margin. *Tectonophysics*, 461, 228–239.
- 763 Cigolini, C. (1995). Geology of the Internal Zone of the Grand Saint Bernard Nappe: a metamorphic Late  
764 Paleozoic volcano-sedimentary sequence in South-Western Aosta Valley (Western Alps). *Boll. Mus.  
765 Reg. Sci. Nat., Torino*, 13(2), 293-327.
- 766 Cocherie, A., Rossi, P., Fouillac, A. M., & Vidal, P. (1994). Crust and mantle contributions to granite  
767 genesis—an example from the Variscan batholith of Corsica, France, studied by trace element and Nd–  
768 Sr–O isotope systematics. *Chem. Geol.*, 115, 173-211.
- 769 Compston, W., Williams, I. S., Kirschvink, J. L., Zhang, Z., & Ma, G. (1992). Zircon U-Pb ages for the  
770 Early Cambrian time-scale. *J. Geol. Soc. London*, 149, 171-184.
- 771 Corfu, F., Hanchar, J. M., Hoskin, P. W. O., & Kinny, P. D. (2003). Atlas of zircon textures. In J. M.  
772 Hanchar, & P. W. O. Hoskin (Eds.), *Zircon*, (Vol. 53, pp. 469-500). Rev. Mineral. Geochem., Mineral.  
773 Soc. America.
- 774 Cosma, L. (1999). *Géologie et magmatisme paléozoïque en Vanoise septentrionale (La Sauvire, Plan  
775 Richard), implications géodynamiques*, (Diplome Géol Minéral), Lausanne, CH: Univ. of Lausanne.
- 776 Costa, S., & Rey, P. (1995). Lower crustal rejuvenation and growth during post-thickening collapse: Insights  
777 from a crustal cross section through a Variscan metamorphic core complex. *Geology*, 23, 905– 908.
- 778 Dallagiovanna, G., Gaggero, L., Maino, M., Seno, S., & Tiepolo, M. (2009). U-Pb zircon ages for post-  
779 Variscan volcanism in the Ligurian Alps (Northern Italy). *J. Geol. Soc. London*, 166, 101-114.
- 780 Dal Piaz, Gb. (1928). Geologia della catena Herbetet-Grivola-Grand Nomenon. *Mem. Ist. Geol. Univ.  
781 Padova*, 7, 1-84.
- 782 Dal Piaz, Gb. (1939). La discordanza ercina nella zona pennidica e le sue conseguenze nei riguardi della  
783 Storia geologica della Alpi. *Boll. Soc. Geol. It.*, 58, 105-152.
- 784 Dal Piaz, G. V. (1965). Il lembo di ricoprimento della Becca di Toss: struttura retroflessa del Gran San  
785 Bernardo. *Mem. Acc. Patavina SS. LL. AA.*, 77 (1964-65), 107-136.

- 786 Dal Piaz, G. V. (1993). Evolution of Austro-Alpine and Upper Penninic basement in the northwestern Alps  
787 from Variscan convergence to post-Variscan extension. In J. von Raumer, F. Neubauer (Eds.), *Pre-*  
788 *Mesozoic Geology in the Alps*. (pp. 327-344). Heidelberg, D: Springer-Verlag.
- 789 Dal Piaz, G. V., & Govi, M. (1965). Osservazioni geologiche sulla "Zona del Gran San Bernardo" nell'alta  
790 Valle d'Aosta. *Boll. Soc. Geol. It.*, 84(1), 1-25.
- 791 Dal Piaz, G. V., & Martin, S. (1998). Evoluzione litosferica e magmatismo nel dominio austro-sudalpino  
792 dall'orogenesi varisica al rifting permo-mesozoico. *Mem. Soc. Geol. It.*, 53, 43-62.
- 793 Dal Piaz, G. V., De Vecchi, Gp, & Hunziker, J. C. (1977). The Austroalpine layered gabbros of the  
794 Matterhorn and Mt.Collon-Dents de Bertol. *Schweiz. Miner. Petrogr.*, 57, 59-88.
- 795 Dal Piaz, G.V., Bistacchi, A., & Massironi, M. (2003). Geological outline of the Alps. *Episodes*, 26(3), 174-  
796 179.
- 797 Debemas, J., and R. Caby avec la collaboration de P. Antoine, G. Elter, P. Elter, M. Govi, J. Fabre, T.  
798 Baudin, R. Marion, E. Jaillard, D. Mercier, and F. Guillot (1991), Feuille Sainte-Foy-Tarentaise (728)  
799 et Notice explicative, Carte géologique France (1/50 000), 43 pp., BRGM, Orleans.
- 800 Debon, F., & Lemmet, M. (1999). Evolution of Mg/Fe ratios in Late Variscan plutonic rocks from the  
801 External Crystalline Massifs of the Alps (France, Italy, Switzerland). *J. Petrol.*, 40, 1151-1185.
- 802 De Giusti, F., Dal Piaz, G. V., Massironi, M., & Schiavo, A. (2004). Carta geotettonica della Valle d'Aosta.  
803 *Mem. Sci. Geol.*, 55 (2003), 129-149.
- 804 De la Roche, H., Leterrier, J., Granclaude, P., & Marchal, M. (1980). A classification of volcanic and  
805 plutonic rocks using R1R2-diagram and major-element analyses - its relationships with current  
806 nomenclature. *Chemical Geology*, 29, 183-210.
- 807 Derron, M. H., Jacquod, J., & Sartori, M. (2006). The Goli d'Aget Member: Early Permian volcanoclastic  
808 and volcanic rocks within the Briançonnais Grand St-Bernard Nappe (Valais, Switzerland). *Eclogae  
809 Geol. Helv.*, 99, 301-307.
- 810 Desmons, J. (1992). The Briançon basement (Penninic Western Alps): mineral composition and  
811 polymetamorphic evolution. *Schweiz. Miner. Petrogr.*, 72, 37-55.
- 812 Desmons, J., & Mercier, D. (1993). Passing through the Briançon zone. In J. von Raumer, F. Neubauer  
813 (Eds.), *Pre-Mesozoic Geology in the Alps*. (pp. 279-295). Heidelberg, D: Springer-Verlag.
- 814 Desmons, J., Aprahamian, J., Compagnoni, R., Cortesogno, L., & Frey, M. (1999a). Alpine metamorphism of  
815 the Western Alps: I Middle to high-P/T metamorphism. *Schweiz. Miner. Petrogr.*, 79, 89-110.
- 816 Desmons, J., Compagnoni, R., Cortesogno, L., Frey, M., & Gaggero, L. (1999b). Pre-Alpine metamorphism  
817 of the Internal zones of the Western Alps. *Schweiz. Miner. Petrogr.*, 79, 23-39.
- 818 Détraz, G., & Loubat, H. (1984). Facies à disthène, staurotide et grenat dans un micaschiste appartenant à  
819 l'unité des "Gneiss du Sapey" (Vanoise, Alpes françaises). *Geol. Alpine*, 60, 5-12.
- 820 Duchesne, J-C, Liégeois, J-P, Bolle, O., Vander Auwera, J., Bruguier, O., Matukov, D.I., & Sergeev, S.A.  
821 (2013). The fast evolution of a crustal hot zone at the end of a transpressional regime: The Saint-Tropez  
822 peninsula granites and related dykes (Maures Massif, SE France). *Lithos*, 162-163, 195-220.
- 823 Edel, J. B., Schulmann, K., Skrzypek, E., & Cocherie, A. (2013). Tectonic evolution of the European  
824 Variscan belt constrained by palaeomagnetic, structural and anisotropy of magnetic susceptibility data  
825 from the Northern Vosges magmatic arc (eastern France). *J. Geol. Soc. London*, 170, 785-804.
- 826 Eichhorn, R., Loth, G., Holl, R., Finger, F., Schermaier, A., & Kennedy, A. (2000). Multistage Variscan  
827 magmatism in the central Tauern Window (Austria) unveiled by U/Pb SHRIMP zircon data. *Contrib.  
828 Mineral. Petrol.*, 139, 418-435.
- 829 Ellenberger, F. (1958). Etude géologique du pays de Vanoise, Mém. Pour servir à l'explication se la Carte  
830 géol. détaillée de la France, 561 pp.
- 831 Elter, G. (1987). Carte géologique de la Vallée d'Aoste. Firenze, I: SELCA.

- 832 Escher, A., Masson, H., & Steck, A. (1993). Nappe geometry in the Western Swiss Alps. *J. Struct. Geol.*, 15,  
833 501-509.
- 834 Fabre, J. (1958). *Contribution à l'étude de la zone Houillère en Maurienne et en Tarentaise (Alpes de*  
835 *Savoie)*. (PhD thesis). Paris, F: Faculté des Sciences de l'Université de Paris.
- 836 Faure, M., Bé Mézème, E., Duguet, M., Cartier, C., & Talbot, J. (2005). Paleozoic tectonic evolution of  
837 medio-Europa from the example of the French Massif Central and Massif Armorican. In R. Carosi, R.  
838 Dias, D. Iacopini, G. Rosenbaum (Eds.), *The southern Variscan belt* (Vol. 19, paper 5). J. Virtual  
839 Explorer, doi:10.3809/jvirtex.2005.00120.
- 840 Finger, F., & Steyrer, H. P. (1995). A tectonic model for the eastern Variscides: indications from a chemical  
841 study of amphibolites in the south-eastern Bohemian Massif. *Geol. Carpathica*, 46, 137-150.
- 842 Flisch, M. (1987). *Teil 1: Geologische, petrographische und isotopengeologische Untersuchungen an*  
843 *Gesteinen des Silvrettkristallins, Teil 2: Die Hebungs geschichte der oberostalpinen Silvretta-Decke*  
844 *seit der mittleren Kreide*. (PhD Thesis). Berne, CH: Universität.
- 845 Floyd, P.A., Winchester, J., Seston, R., Kryza, R., & Crowley, Q. G. (2000). Review of geochemical  
846 variation in lower Palaeozoic metabasites from the NE Bohemian Massif: intracratonic rifting and  
847 plume-ridge interaction, in Orogenic processes - quantification and modelling. In W. Franke, R.  
848 Altherr, V. Haak, O. Oncken, D. Tanner (Eds.), *The Variscan belt of Central Europe* (Vol. 179, pp.155-  
849 174). Sp. Publ., Geol. Soc. London.
- 850 Franchi, S., & Stella, A. (1903) I giacimenti di antracite della Valle d'Aosta. *Mem. descr. Carta Geol. It.*, 12,  
851 11-92.
- 852 Friedl, G., Finger, F., Paquette, J. L., von Quadt, A., McNaughton, N. J., & Fletcher, I. R. (2004). Pre-  
853 Variscan geological events in the Austrian part of the Bohemian Massif deduced from U-Pb zircon  
854 ages. *Int. J. Earth Sci.*, 93, 802-823.
- 855 Frost, B. R., Barnes, C. G., Collins, W. J., Arculus, R. J., Ellis, D. J., & Frost, C. D. (2001). A geochemical  
856 classification for granitic rocks. *J. Petrol.*, 42, 2033-2048.
- 857 Gaggero, L., Cortesogno, L., & Bertrand, J. M. (2004). The pre-Namurian basement of the Ligurian Alps.  
858 *Period. Mineral.*, 73, 85-96.
- 859 Galli, A., Le Bayon, B., Schmidt, M. W., Burg, J. P., Reusser, E. S., Sergeev, A. & Larionov, A. (2012). U-  
860 Pb zircon dating of the Gruf Complex: disclosing the late Variscan granulitic lower crust of Europe  
861 stranded in the Central Alps. *Contrib. Mineral. Petrol.*, 163, 353-378.
- 862 Gauthiez, L., Bussy, F., Ulianov, A., Gouffon, Y., & Sartori, M. (2011). Ordovician mafic magmatism in the  
863 Me'tailleur Formation of the Mont-Fort nappe (Middle Penninic domain, western Alps) - Geodynamic  
864 implications. 9th Swiss Geoscience Meeting, Zurich, CH.
- 865 Gebauer, D., Schertl, H. P., Brix, M., & Schreyer, W. (1997). 35 Ma old ultrahigh-pressure metamorphism  
866 and evidence for rapid exhumation in the Dora Maira Massif, Western Alps. *Lithos*, 41, 5-24.
- 867 Genier, F., Epard, J. L., Bussy, F., & Magna, T. (2008). Lithostratigraphy and U-Pb zircon dating in the  
868 overturned limb of the Siviez-Mischabel nappe: a new key for Middle Penninic nappe geometry. *Swiss*  
869 *J. Geosci.*, 101, 431-452.
- 870 Giacomini, F., Braga, R., Tiepolo, M., & Tribuzio, R. (2007). New constraints on the origin and age of  
871 Variscan eclogitic rocks (Ligurian Alps, Italy). *Contrib. Mineral. Petrol.*, 153, 29-53.
- 872 Giorgis, D., Thelin, P., Stampfli, G., & Bussy, F. (1999). The Mont-Mort metapelites: Variscan  
873 metamorphism and geodynamic context (Briançonnais basement, Western Alps, Switzerland). *Schweiz.*  
874 *Miner. Petrogr.*, 79, 381-398.
- 875 Gouffon, Y. (1993). Géologie de la "nappe" du Grand St-Bernard entre la Doire Baltée et la frontière suisse  
876 (Vallée d'Aoste - Italie). *Mémoires de Géologie Lausanne*, 12, 1-147.
- 877 Govi, M. (1966). Contributo alla conoscenza della zona mesozoica di Avise (alta val d'Aosta). *Boll. Soc.*  
878 *Geol. It.*, 85, 705-719.

- 879 Gretter, N., Ronchi, A., Langone, A., & Perotti, C. (2013). The transition between the two major Permian  
880 tectono-stratigraphic cycles in the central Southern Alps: results from facies analysis and U/Pb  
881 geochronology. *Int. J. Earth Sci.*, 102, 1181-1202.
- 882 Grujic, D., & Mancktelow N.S (1996). Structure of the northern Maggia and Lebendun Nappes, Central Alps,  
883 Switzerland. *Eclogae Geol. Helv.*, 89, 461-504.
- 884 Guerrot, C., & Debon, F. (2000). U-Pb dating of two contrasting Late Variscan plutonic suites from the  
885 Pelvoux massif (French Western Alps). *Swiss Bull. Miner. Petrol.*, 80, 249–256.
- 886 Guillot, F., Liegois, J.P., & Fabre, J. (1991). Des granophyres du Cambrien dans le Mont Pourri (Vanoise,  
887 zone briançonnaise): première datation U-Pb sur zircon d'un socle des zones internes des Alpes  
888 francaises. *C.R. Acad. Sci. Paris*, 313, 239-244.
- 889 Guillot, F., Desmons, J., & Ploquin, A. (1993). Lithostratigraphy and geochemical composition of the Mont  
890 Pourri volcanic basement, Middle Penninic W-Alpine zone, France. *Schweiz. Miner. Petrogr.*, 73, 319-  
891 334.
- 892 Guillot, F., Schaltegger, U., Bertrand, J.M., Deloule, E., & Baudin, T. (2002). Zircon U-Pb geochronology of  
893 Ordovician magmatism in the polycyclic Ruitor Massif (Internal W Alps). *Int. J. Earth Sci.*, 91, 964-978.
- 894 Guillot, F., Bertrand, J.M., Bussy, F., Lanari, P., Cosma, L., & Pin, Ch. (2012). Early Variscan I-type pluton  
895 in the pre-Alpine basement of the Western Alps: The ca. 360 Ma Cogne diorite (NW-Italy). *Lithos*,  
896 153, 94-107.
- 897 Guillot, S., & Ménot, R.P. (2009). Paleozoic evolution of the External Crystalline Massifs of the Western  
898 Alps. *C.R. Geosci.*, 341, 253-265.
- 899 Guillot, S., di Paola, S., Ménot, R-P, Ledru, P., Spalla, M.I., Goso, G., & Schwartz, S. (2009). Suture zones  
900 and importance of strike-slip faulting for Variscan geodynamic reconstructions of the External  
901 Crystalline Massifs of the western Alps. *Bull. Soc. Géol. Fr.*, 180, 483–500.
- 902 Handy, M.R., Schmid, S.M., Bousquet, R., Kissling, E., & Bernoulli, D. (2010). Reconciling plate-tectonic  
903 reconstructions of Alpine Tethys with the geological-geophysical record of spreading and subduction in  
904 the Alps. *Earth Sci. Rev.*, 102, 121–158.
- 905 Hatcher, Jr. R.D. (2002). Alleghanian (Appalachian) orogeny, a product of zipper tectonics: rotational  
906 transpressive continent-continent collision and closing of ancient oceans along irregular margins. In  
907 J.R. Martínez Catalán, R.D. Hatcher Jr., R. Arenas, F. Díaz García (Eds.), *Variscan-Appalachian*  
908 *dynamics: The building of the Late Paleozoic basement* (Vol. 364, pp. 199–208). Sp. Paper, Geol. Soc.  
909 America.
- 910 Hawkesworth, C., Turner, S., Gallagher, K., Hunter, A., Bradshaw, T., & Rogers, N. (1995). Calc-alkaline  
911 magmatism, lithospheric thinning and extension in the Basin and Range. *J. Geophys. Res.*, 100, 10271-  
912 10286.
- 913 Hoskin, P.W.O., & Schaltegger, U. (2003). The composition of zircon and igneous and metamorphic  
914 petrogenesis. In J.M. Hanchar, P.W.O. Hoskin (Eds.), *Zircon* (Vol. 53, pp. 27-62). Rev. Mineral.  
915 Geochem., Mineral. Soc. of America.
- 916 Janousek, V., Bowes, D.R., Rogers, G., Farrow, C.M., & Jelinek, E. (2000). Modeling diverse processes in  
917 the petrogenesis of a composite batholith: the Central Bohemian Pluton, Central European Hercynides.  
918 *J. Petrol.*, 41, 511-543.
- 919 Janousek, V., Braithwaite, C.J.R., Bowes, D.R., & Gerdes, A. (2004). Magma mixing in the genesis of  
920 Hercynian calc-alkaline granitoids: an integrated petrographic and geochemical study of the Sazava  
921 intrusion, Central Bohemian Pluton, Czech Republic. *Lithos*, 78, 67-99.
- 922 Kosler, J., Rogers, G., Roddick, J.C., & Bowes, D.R. (1995). Temporal association of ductile deformation  
923 and granitic plutonism: Rb-Sr and 40Ar-39Ar evidence from roof pendants above the Central  
924 Bohemian Pluton, Czech Republic. *J. Geol.*, 103, 711-717.

- 925 Kroner, U., & Romer, R.L. (2013). Two plates - Many subduction zone: The Variscan orogeny reconsidered.  
926 *Gondwana Res.*, 24, 298-329.
- 927 Ladenhauf, C., Armstrong, R., Konzett, J., & Miller, C. (2001). The timing of pre-Alpine high pressure  
928 metamorphism in the Eastern Alps: constraints from U-Pb SHRIMP dating of eclogite zircons from the  
929 Austroalpine Silvretta nappe. *J. Conference Abstracts (EUG XI)*, 6, pp. 600.
- 930 Liati, A., Gebauer, D., & Fanning, M. (2009). Geochronological evolution of HP metamorphic rocks of the Adula  
931 nappe, Central Alps, in pre-Alpine and Alpine subduction cycles. *J. Geol. Soc. London*, 166, 797-810.
- 932 Liati, A., Gebauer, D., & Froitzheim, N. (2001). U-Pb SHRIMP geochronology of an amphibolitized  
933 eclogite and an orthogneiss from Furg zone (Western Alps) and implications for its geodynamic  
934 evolution. *Schweiz. Miner. Petrogr.*, 81, 379-393.
- 935 Ludwig, K.R. (1998). On the treatment of concordant uraniumlead ages. *Geochim. Cosmochim. Acta*, 62, 665-676.
- 936 Ludwig, K.R. (2003a). SQUID 1.02: A User's Manual. Berkeley Geochronological Center, Spec. Publ. 2.
- 937 Ludwig, K.R. (2003b). A User's Manual for Isoplot/Ex 3: A Geochronological Toolkit for Microsoft Excel.  
938 Berkeley Geochronological Center, Spec. Publ. 4.
- 939 Malusà, M.G., Polino, R., & Martin, S. (2005a). The Gran San Bernardo nappe in the Aosta valley (western  
940 Alps): a composite stack of distinct continental crust units. *Bull. Soc. Geol. Fr.*, 176(5), 417-431.
- 941 Malusà, M.G., Polino, R., Zattin, M., Bigazzi, G., Martin, S., & Piana, F. (2005b). Miocene to present  
942 differential exhumation in the Western Alps: Insights from fission track thermochronology. *Tectonics*,  
943 24, 1-23.
- 944 Malusà, M.G., Polino, R., & Zattin, M. (2009). Strain partitioning in the axial NW Alps since the Oligocene.  
945 *Tectonics*, 28, 1-26.
- 946 Malusà, M.G., Faccenna, C., Garzanti, E., & Polino, R. (2011). Divergence in subduction zones and  
947 exhumation of high-pressure rocks (Eocene Western Alps). *Earth Planet. Sci. Lett.*, 310, 21-32.
- 948 Malusà, M.G., Faccenna, C., Baldwin, S.L., Fitzgerald, P.G., Rossetti, F., Balestrieri, M.L., Danišk, M.,  
949 Ellero, A., Ottria, G., & Piromallo, C. (2015). Contrasting styles of (U)HP rock exhumation along the  
950 Cenozoic Adria-Europe plate boundary (Western Alps, Calabria, Corsica). *Geochem. Geophys. Geosyst.*, 16, 1786-1824.
- 952 Malusà, M.G., Danišk, M., & Kuhleman, J. (2016). Tracking the Adriatic-slab travel beneath the Tethyan  
953 margin of Corsica-Sardinia by low-temperature thermochronometry. *Gondwana Res.*, 31, 135-149
- 954 Manzotti, P., Pouiol, M., & Ballèvre, M. (2015). Detrital zircon geochronology in blueschist-facies meta-  
955 conglomerates from the Western Alps: implications for the late Carboniferous to early Permian  
956 palaeogeography. *Int. J. Earth Sci.*, 104, 703-731.
- 957 Manzotti, P., Ballèvre, M., & Pouiol, M. (2016). Detrital zircon geochronology in the Dora-Maira and Zone  
958 Houillere: a record of sediment travel paths in the Carboniferous. *Terra Nova*, doi: 10.1111/ter.12219.
- 959 Manzotti, P., Ballèvre, M., & Dal Piaz, G.V. (2017). Continental gabbros in the Dent Blanche Tectonic  
960 System (Western Alps): from the pre-Alpine crustal structure of the Adriatic palaeo-margin to the  
961 geometry of an alleged subduction interface. *J. Geol. Soc.*, doi: 10.1144/jgs2016-071
- 962 Markley, M.J., Teyssier, C., Cosca, M.A., Caby, R., Hunziker, J.C., & Sartori, M. (1998). Alpine  
963 deformation and  $^{40}\text{Ar}/^{39}\text{Ar}$  geochronology of sinkinematic white mica in the Siviez-Mischabel nappe,  
964 western Pennine Alps, Switzerland. *Tectonics*, 17, 407-425.
- 965 Marotta, A.M., & Spalla, M.I. (2007). Permian-Triassic high thermal regime in the Alps: Result of late  
966 Variscan collapse or continental rifting? Validation by numerical modeling. *Tectonics*, 26 (4), TC4016.
- 967 Marquer, D., Challandes, N., & Schaltegger, U. (1998). Early Permian magmatism in Briançonnais terranes:  
968 Truzzo granite and Roffna rhyolite (eastern Penninic nappes, Swiss and Italian Alps). *Schweiz. Miner. Petrogr.*, 78, 397-414.

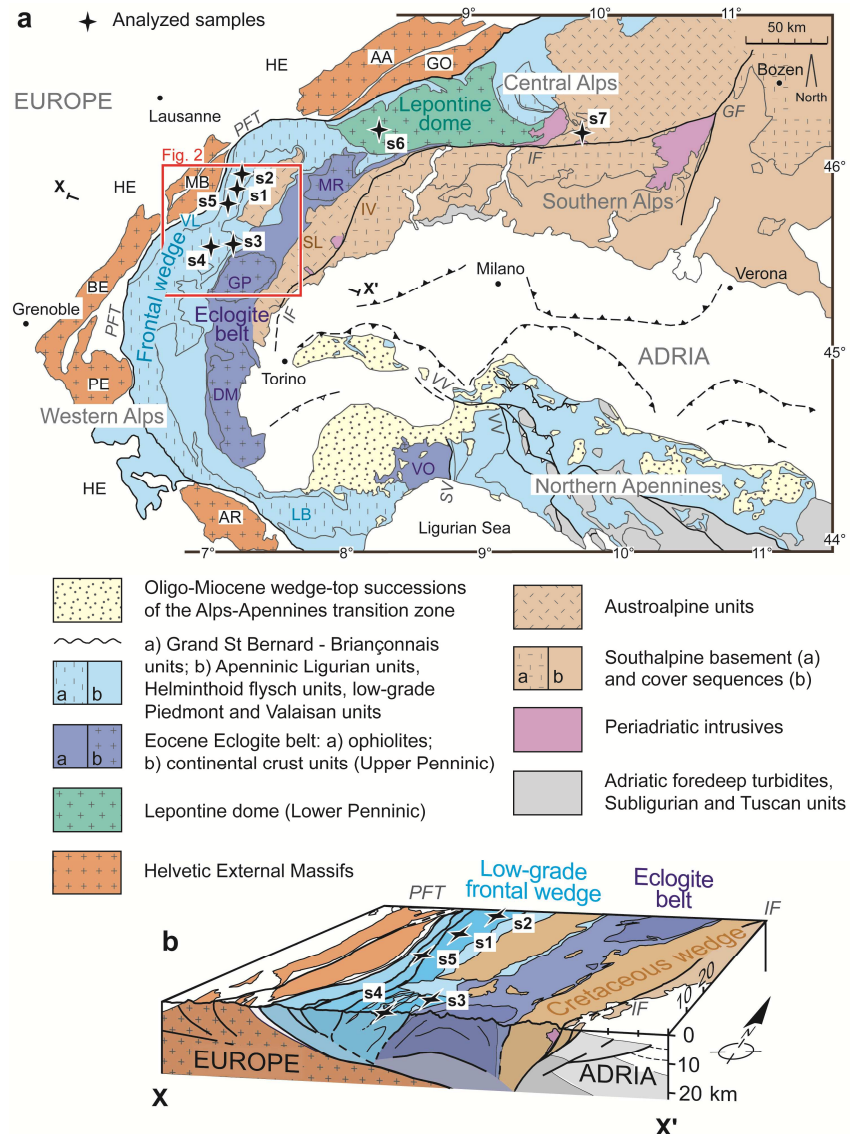
- 970 Martinez Catalan, R., Perez Estaun, A., Bastida, F., & Pulgar, J.A. (1990). West Asturian-Leonese Zone  
971 Structure. In R. D. Dallmeyer, E. Martinez Garcia (Eds.), *Pre-Mesozoic Geology of Iberia* (pp. 103-  
972 114). Springer-Verlag, Heidelberg.
- 973 Matte, Ph. (2001). The Variscan collage and orogeny (480-290 Ma) and the tectonic definition of the  
974 Armorica microplate: a review. *Terra Nova*, 13, 122-128.
- 975 Matte, Ph., Maluski, H., Rajlich, P., & Franke, W. (1990). Terrane boundaries in the Bohemian massif:  
976 result of large-scale Variscan shearing. *Tectonophysics*, 177, 151-170.
- 977 Maxelon, M., & Mancktelow, N.S (2005). Three-dimensional geometry and tectonostratigraphy of the  
978 Pennine zone, Central Alps, Switzerland and Northern Italy. *Earth-Sci. Rev.*, 71, 171-227.
- 979 Melcher, F., & Meisel, T. (2004). A metamorphosed Early Cambrian crust-mantle transition in the Eastern  
980 Alps, Austria. *J. Petrol.*, 48, 1689-1723
- 981 Melleton, J., Cocherie, A., Faure, M., Rossi, P., & Arenas, R. (2010). Precambrian protoliths and Early  
982 Paleozoic magmatism in the French Massif Central: U-Pb data and the North Gondwana connection in  
983 the west European Variscan belt. *Gondwana Res.*, 17, 13-25.
- 984 Ménot, R-P., Peucat, J.J., Scarenzi, D., & Piboule, M. (1988). 496 My age of plagiogranites in the  
985 Chamrousse ophiolite complex (External Crystalline Massifs in the French Alps): evidence of a Lower  
986 Paleozoic oceanisation. *Earth Planet. Sci. Lett.*, 88, 82-92.
- 987 Miller, C., & Thöni, M. (1995). Origin of eclogites from the Austroalpine Ötztal basement (Tirol, Austria):  
988 geochemistry and Sm-Nd vs. Rb-Sr isotope systematics. *Chem. Geol.*, 122, 199-225.
- 989 Milnes, A.G. (1974). Structure of the Pennine Zone (Central Alps): A New Working Hypothesis. *Geol. Soc.  
990 Am. Bull.*, 85, 1727-1732.
- 991 Muttoni, G., Kent, D.V., Garzanti, E., Brack, P., Abrahamsen, N., & Gaetani, M. (2003). Early Permian  
992 Pangea 'B' to Late Permian Pangea 'A'. *Earth Planet. Sci. Lett.*, 215, 379-394.
- 993 Nangeroni, G. (1957). La struttura geologica del territorio della provincia di Sondrio. *Ed. Amm. Prov.  
994 Sondrio*.
- 995 Nasdala, L., Hofmeister, W., Norberg, N., Mattinson, J.M., Corfu, F., Dörr, W., Kamo, S.L., Kennedy, A.K.,  
996 Kronz, A., Reiners, P.W., Frei, D., Kosler, J., Wan, Y., Götze, J., Häger, T., Kröner, A., & Valley, J.W.  
997 (2008). Zircon M257 - a homogeneous natural reference material for the ion microprobe U-Pb analysis  
998 of zircon. *Geostand. Geoanal. Res.*, 32, 247-265.
- 999 Neubauer, F. (2002). Evolution of Late Neoproterozoic to Early Paleozoic tectonic elements in Central and  
1000 Southeast European Alpine mountain belts: review and synthesis. *Tectonophysics*, 352, 87-103.
- 1001 Neubauer, F., & Handler, R. (1999). Variscan orogeny in the Eastern Alps and Bohemian Massif: How do  
1002 these units correlate?. *Mitt. Osterr. Geol. Ges.*, 92, 35-39.
- 1003 Neubauer, F., Frisch, W., & Hansen, B.T. (2003). Early Paleozoic and Variscan Events in the Austroalpine  
1004 Rennfeld Block (Eastern Alps): A U-Pb Zircon Study. *Jb. Geol. B.-A.*, 143, 567-580.
- 1005 Notarpietro, A., & Gorla, L. (1981). Contributo alla conoscenza delle formazioni austriache nell'alta e  
1006 media Valtellina. Variazioni petrochimiche nella Formazione di Valle Grosina. *Rend. Soc. It. Min.  
1007 Petr.*, 37, 755-791, 1981.
- 1008 Novarese, V. (1909). Il profilo della Grivola (Alpi Graie). *Boll. R. Com. Geol. It.*, 40, 497-525.
- 1009 Oberli, F., Meier, M., & Biino, G.G. (1994). Time constraints on the pre-Variscan agmatic-metamorphic  
1010 evolution of the Gotthard and Tavetsch units derived from single-zircon U-Pb results. *Schweiz. Miner.  
1011 Petrogr.*, 74, 483-488.
- 1012 Oggiano, G., Casini, L., Mameli, P., & Rossi, P. (2007). Long lived dextral strike-slip tectonics in the  
1013 southern Variscan Belt: evidence from two syn-kynematic intrusions in north Sardinia. *Geol. Fr.*, 2,  
1014 142.
- 1015 Pace, E. (1966). Studio petrografico dell'alta Val Viola (Sondrio). *Atti Soc. It. Sc. Nat.*, 105, 43-60.

- 1016 Paquette, J-L, Chopin, C., & Peucat, J-J (1989). U-Pb zircon, and Rb-Sr and Sm-Nd geochronology of high-  
1017 to very- high-pressure meta-acidic rocks from western Alps. *Contrib. Mineral. Petr.*, 101, 280-289.
- 1018 Paquette, J-L, Ménot, R-P, Pin, C., & Orsini, J.B. (2003). Episodic and short-lived granitic pulses in a post-  
1019 collisional setting: evidence from precise U–Pb zircon dating through a crustal cross-section in Corsica.  
1020 *Chem. Geol.*, 198, 1-20.
- 1021 Pawlig, S., & Baumgartner, L. (2001). Geochemistry of talc-kynite-chloritoid shear zone within the Monte  
1022 Rosa granite, Val d'Ayas, Italy. *Schweiz. Miner. Petrogr.*, 81, 329-346.
- 1023 Peccerillo, A., & Taylor, S.R. (1976). Geochemistry of Eocene calc-alkaline volcanic rocks from Kastamonu  
1024 area, Northern Turkey. *Contrib. Mineral. Petr.*, 58, 63-81.
- 1025 Pezzotta, F., & Pinarelli, L. (1994). The magmatic evolution of Ordovician metagranitoids of the Serie dei  
1026 Laghi (Southern Alps): inferences from petrological, geochemical, and Sr and Nd isotope data. *Period.  
1027 Mineral.*, 63, 127-147.
- 1028 Pin, C. & Paquette, J-L (2002). Sr-Nd isotope and trace element evidence for a Late Deonian active margin  
1029 in northern Massif Central (France). *Geodin. Acta*, 15, 63-77.
- 1030 Pinarelli, L., Del Moro, A., & Boriani, A. (1988). Rb-Sr geochronology of Lower Permian plutonism in  
1031 Massiccio dei Laghi, Southern Alps (NW Italy). *Rend. Soc. Ital. Mineral. Petr.*, 43, 411-428.
- 1032 Pinarelli, L., & Boriani, A. (2007). Tracing metamorphism, magmatism and tectonics in the southern Alps  
1033 (Italy): constraints from Rb-Sr and Pb-Pb geochronology, and isotope geochemistry. *Period. Mineral.*,  
1034 76, 5-24.
- 1035 Polino, R., Malusà, M.G., Martin, S., Carraro, F., Gianotti, F., et al. (2015). Foglio 090 Aosta e Note  
1036 illustrative, Carta Geologica d'Italia alla scala 1:50.000, ISPRA.
- 1037 Poller, U. (1997). U-Pb single-zircon study of gabbroic and granitic rocks in the Val Barlasch (Silvretta  
1038 nappe, Switzerland). *Schweiz. Miner. Petrogr.*, 77, 351–360.
- 1039 Ring, U., Collins, A., & Kassem, O.K. (2005). U-Pb SHRIMP data on the crystallization age of the Gran  
1040 Paradiso augengneiss, Italian Western Alps: further evidence for Permian magmatic activity in the Alps  
1041 during break-up of Pangea. *Eclogae Geol. Helv.*, 98, 363-370.
- 1042 Rode, S., Rösel, D., & Schulz, B. (2012). Constraints on the Variscan P-T evolution by EMP Th-U-Pb  
1043 monazite dating in the polymetamorphic Austroalpine Oetztal-Stubai basement (eastern Alps),  
1044 *Zeitschrift Deutsh. Ges. Geowiss.*, 163, 43-67.
- 1045 Rolland, Y., Corsini, M., & Demoux, A. (2009). Metamorphic and structural evolution of the Maures–  
1046 Tanneron massif (SE Variscan chain): evidence of doming along a transpressional margin. *Bull. Soc.  
1047 Géol. France*, 180, 217–230.
- 1048 Rosenbaum, G., & Lister, G.S. (2005). The Western Alps from the Jurassic to Oligocene: spatio-temporal  
1049 constraints and evolutionary reconstructions. *Earth Sci. Rev.*, 69, 281-306.
- 1050 Rossi, P., Oggiano, G., & Cocherie, A. (2009). A restored section of the “southern Variscan realm” across  
1051 the Corsica-Sardinia microcontinent. *C.R. Geosci.*, 341, 224-238.
- 1052 Rubatto, D., Schaltegger, U., Lombardo B., & Compagnoni, R. (2001). Complex Paleozoic magmatic and  
1053 metamorphic evolution in the Argentera Massif (Western Alps) resolved with U–Pb dating. *Schweiz.  
1054 Miner. Petrogr.*, 81, 213–228.
- 1055 Rubatto, D., Ferrando, S., Compagnoni, R., & Lombardo, B. (2010). Carboniferous high-pressure  
1056 metamorphism of Ordovician protholiths in the Argentera Massif (Italy), Southern European Variscan  
1057 belt. *Lithos*, 116, 65-76.
- 1058 Sanchez Garcia, T., Bellido, F., & Quesada, C. (2003). Geodynamic setting and geochemical signatures of  
1059 Cambrian–Ordovician rift-related igneous rocks (Ossa-Morena zone, SW Iberia). *Tectonophysics*, 365,  
1060 233-255.

- 1061 Sartori, M., Gouffon, Y., & Marthaler, M. (2006). Harmonisation et définition des unités  
1062 lithostratigraphiques briançonnaises dans les nappes penniques du Valais. *Eclogae Geol. Helv.*, 99, 363-  
1063 407.
- 1064 Schaltegger, U. (1994). Unravelling the pre-Mesozoic history of Aar and Gotthard massifs (Central Alps) by  
1065 isotopic dating: a review. *Schweiz. Miner. Petrogr.*, 74, 41-51.
- 1066 Schaltegger, U. (2000). U-Pb geochronology of the Southern Black Forest batholith (Central Variscan Belt):  
1067 timing of exhumation and granite emplacement. *Int. J. Earth Sci.*, 88, 814-828.
- 1068 Schaltegger, U., & Brack, P. (1999). Short-lived events of extension and volcanism in the Lower Permian of  
1069 the Southern Alps (northern Italy, southern Switzerland). *J. Conf. Abstr.*, 4(1), 296-297.
- 1070 Schaltegger, U., & Brack, P. (2007). Crustal-scale magmatic systems during intracontinental strike-slip  
1071 tectonics: U, Pb and Hf isotopic constraints from Permian magmatic rocks of Southern Alps. *Int. J.*  
1072 *Earth Sci.*, 96, 1131-1151.
- 1073 Schaltegger, U., & Gebauer, D. (1999). Pre-Alpine geochronology of the central, western and southern Alps.  
1074 *Schweiz. Miner. Petrogr.*, 79, 79-87.
- 1075 Schaltegger, U., Nagler, Th.N., Corfu, F., Megetti, M., Galetti, G., & Stosch, H.G. (1997). A Cambrian  
1076 island arc in the Silvretta nappe: constraints from geochemistry and geochronology. *Schweiz. Miner.*  
1077 *Petrogr.*, 77, 337-350.
- 1078 Schaltegger, U., Abrecht, J., & Corfu, F. (2003). The Ordovician orogeny in the Alpine basement:  
1079 constraints from geochronology and geochemistry in the Aar Massif (Central Alps). *Schweiz. Miner.*  
1080 *Petrogr.*, 83, 183-195.
- 1081 Scheiber, T., Berndt, J., Heredia, B.D., Mezger, K., & Pfiffner, O.A. (2013). Episodic and long-lasting  
1082 Paleozoic felsic magmatism in the pre-Alpine basement of the Suretta nappe (eastern Swiss Alps). *Int.*  
1083 *J. Earth Sci.*, 102, 2097-2115.
- 1084 Scheiber, T., Berndt, J., Mezger, K., & Pfiffner, O.A. (2014). Precambrian to Paleozoic zircon record in the  
1085 Siviez-Mischabel basement (western Swiss Alps). *Swiss J. Geosci.*, 107, 49-64.
- 1086 Schiavo, A. (1997). *Evoluzione tettonica e metamorfica del massiccio del Ruitor*. PhD Thesis, Geoscience,  
1087 Università di Padova.
- 1088 Schmid S.M., Zingg, A., & Handy, M. (1987). The kinematics of movements along the Insubric Line and  
1089 the emplacement of the Ivrea Zone. *Tectonophysics*, 135, 47-66.
- 1090 Schmid, S. M., Fügenschuh, B., Kissling, E., & Schuster, R. (2004). Tectonic map and overall architecture  
1091 of the Alpine orogen. *Eclogae Geol. Helv.*, 97(1), 93-117.
- 1092 Schöne, B., Crowley, J.L., Condon, D.J., Schmitz, M.D., & Bowring, S.A. (2006). Reassessing the uranium  
1093 decay constants for geochronology using ID-TIMS U-Pb data. *Geochim. Cosmochim. Ac.*, 70, 426-445.
- 1094 Schulz, B., Steenken, A., & Siegesmund, S. (2008). Geodynamic evolution of an Alpine terrane - The  
1095 Austroalpine basement to the south of the Tauern Window as a part of the Adriatic plate (eastern Alps).  
1096 In S. Siegesmund, B. Fügenschuh, N. Froitzheim (Eds), *Tectonic Aspects of the Alpine-Dinaride-*  
1097 *Carpathian System* (Vol. 298, pp. 5-44). Sp. Publ., Geol. Soc. London.
- 1098 Schuster, R., & Stüwe, K. (2008). Permian metamorphic event in the Alps. *Geology*, 36, 603-606.
- 1099 Shaw, A., Downes, H., & Thirlwall, M. F. (1993). The quartz-diorites of Limousin: elemental and isotopic  
1100 evidence for Devono-Carboniferous subduction in the Hercynian belt of the French Massif Central.  
1101 *Chem. Geol.*, 107, 1-18.
- 1102 Shelley, D., & Bossiere, G. (2000). A new model for the Hercynian orogen of Gondwanan France and  
1103 Iberia. *J. Struct. Geol.*, 22, 757-776.
- 1104 Spalla, M.I., Zanoni, D., Marotta, A.M., Rebay, G., Roda, M., Zucali, M., & Goso, G. (2014). The  
1105 transition from Variscan collision to continental break-up in the Alps: insights from the comparison  
1106 between natural data and numerical model predictions. In K. Schulmann, K., J.R. Martínez Catalán,

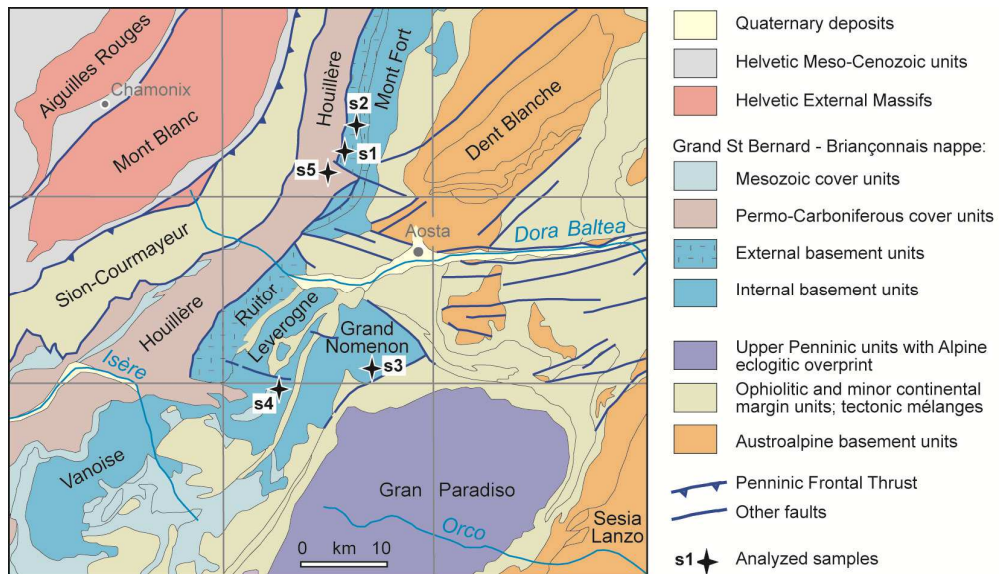
- 1107 J.M. Lardeaux, V. Janoušek, G. Oggiano (Eds.), *The Variscan Orogeny: Extent, Timescale and the*  
1108 *Formation of the European Crust* (Vol. 405, pp. 363-400). Sp. Publ., Geol. Soc. London.
- 1109 Spillmann, P., & Büchi, H.J. (1993). The Pre-Alpine Basement of the Lower Austro-Alpine Nappes in the  
1110 Bernina Massif (Grisons, Switzerland; Valtellina, Italy). In J.F. von Raumer, F. Neubauer (Eds), *Pre-*  
1111 *Mesozoic Geology in the Alps* (pp. 457- 467). Springer-Verlag Berlin Heidelberg.
- 1112 Stacey, J.S., & Kramers, J.D. (1975). Approximation of terrestrial lead evolution by a two-stage model.  
1113 *Earth Planet. Sci. Lett.*, 26, 207–221.
- 1114 Stampfli, G.M., & Borel, G. D. (2002). A plate tectonic model for the Paleozoic and Mesozoic constrained  
1115 by dynamic plate boundaries and restored synthetic oceanic isochrones. *Earth Planet. Sci. Lett.*, 196,  
1116 17–33.
- 1117 Stampfli, G.M., von Raumer, J., & Wilhem, C. (2011). The distribution of Gondwana derived terranes in the  
1118 early Paleozoi. In J. C. Gutiérrez-Marco, I. Rábano, D. García-Bellido (Eds.), *The Ordovician of the*  
1119 *World* (Vol.14, pp. 567–574). Cuadernos del Museo Geominero, Instituto Geológico y Minero de  
1120 España, Madrid.
- 1121 Steck, A., Epard, J-L, Escher, A., Gouffon, Y., & Masson, H. (2001). Carte tectonique des Alpes de Suisse  
1122 occidentale et des régions avoisinantes 1:100,000, Notice explicative. Office fédérale des eaux et de la  
1123 géologie, 73 pp., Berne.
- 1124 Steck, A., Della Torre, F., Keller, F., Pfeifer, H-R, Hunziker, J., & Masson, H. (2013). Tectonics of the  
1125 Lepontine Alps: ductile thrusting and folding in the deepest tectonic levels of the Central Alps. *Swiss J.*  
1126 *Geosci.*, 106, 427-450.
- 1127 Steiger, R.H., & Jäger, E. (1977). Subcommission on geochronology: convention on the use of decay  
1128 constants in geo- and cosmochronology. *Earth Planet. Sci. Lett.*, 36, 359-362.
- 1129 Sun, Ss., & McDonough, W. (1989). Chemical and isotopic systematics of ocean basalts: implications for  
1130 mantle composition and processes. In A.D. Saunders, M.J. Norry (Eds.), *Magmatism in the Ocean*  
1131 *Basins* (Vol. 42, pp. 313-345). Spec. Publ., Geol. Soc. London.
- 1132 Tabaud A-S, Whitechurch, H., Rossi, P., Schulmann, K., Guerrot, C., & Cocherie, A. (2014). Devonian-  
1133 Permian magmatic pulses in the northern Vosges Mountains (NE France): result of continuous  
1134 subduction of the Rhenohercynian Ocean and Avalonian passive margin. In K. Schulmann, J. R.  
1135 Martínez Catalán, J. M. Lardeaux, V. Janousek, G. Oggiano (Eds), *The Variscan orogeny: extent,*  
1136 *timescale and the formation of the European crust* (Vol. 405, pp. 197-223). Sp. Publ., Geol. Soc.  
1137 London.
- 1138 Tatsumi, Y., & Eggins, S. (1995). *Subduction zone magmatism*. Blackwell, Oxford.
- 1139 Tera, F., & Wasserburg, G. (1972). U-Th-Pb systematics in three Apollo 14 basalts and the problem of  
1140 initial Pb in lunar rocks. *Earth Planet. Sci. Lett.*, 14, 281-304.
- 1141 Thélin, P., Sartori, M., Burri, M., Gouffon, Y., & Chessex, R. (1993). The pre-Alpine basement of the  
1142 Briançonnais (Wallis, Switzerland). In J. von Raumer, F. Neubauer (Eds.), *The Pre-Mesozoic Geology*  
1143 *of the Alps* (pp. 297-315). Springer, Heidelberg.
- 1144 Thöni, M. (2003). Erratum. Sm–Nd isotope systematics in garnet from different lithologies (Eastern Alps):  
1145 age results, and an evaluation of potential problems for garnet Sm–Nd chronometry. *Chem. Geol.*, 194,  
1146 353-379.
- 1147 Thöny, W.F., Tropper, P., Schennach, F., Krenn, E., Finger, F., Kaindl, R., Bernhard, F., & Hoinkes, G.  
1148 (2008). The metamorphic evolution of migmatites from the Ötztal complex (Tyrol, Austria) and  
1149 constraints on the timing of the pre-Variscan high-T event in the eastern Alps. *Swiss J. Geosci.*, 101,  
1150 111-126.
- 1151 Tommasini, S., Poli, G., & Halliday, A.N. (1995). The role of sediment subduction and crustal growth in  
1152 Hercynian plutonism: isotopic and trace element evidence from the Sardinia–Corsica batholith. *J.*  
1153 *Petrol.*, 36, 1305-1332.

- 1154 Tumiati, S., Thöni, M., Nimis, P., Martin, S., & Mair, V. (2003). Mantle-crust interactions during Variscan  
1155 subduction in the Eastern Alps (Nonsberg-Ulten Zone): geochronology and new petrological  
1156 constraints. *Earth Planet. Sci. Lett.*, 210, 509-526.
- 1157 Venera, Z., Schulmann, K., & Kroner, A. (2000). Intrusion within a transtensional tectonic domain: the Cista  
1158 granodiorite (Bohemian Massif) – structure and rheological modelling. *J. Struct. Geol.*, 22, 1437-1454.
- 1159 Venzo, S., Crespi, R., Schiavinato, G., & Fagnani, G. (1971). Carta geologico-petrografica delle Alpi  
1160 Insubriche Valtellinesi tra la Val Masino e la Val Malenco (Sondrio). *Mem. Soc. It. Sci. Nat.*, 19.
- 1161 Venzo, S., & Schiavinato, G. (1970). Illustrazione riassuntiva della Carta geologico-petrografica delle Alpi  
1162 Insubriche Valtellinesi tra la Val Masino e la Val Malenco (Sondrio), scale 1:25000. *Boll. Soc. Geol. It.*,  
1163 89, 599-602
- 1164 von Quadt, A., Grunefelder, M., & Buchi, H. (1994). U-Pb zircon ages igneous rocks of the Bernina nape  
1165 system (Grisons, Switzerland). *Schweiz. Miner. Petrogr.*, 74, 373-382.
- 1166 von Raumer, J. F. (1981). Variscan events in the Alpine region. *Geol. Mijnbouw*, 60, 67-80.
- 1167 von Raumer, J. F. (1998). The Palaeozoic evolution in the Alps - From Gondwana to Pangea. *Geol.  
1168 Rundsch.*, 87, 407-435.
- 1169 von Raumer, J.F., Stampfli, G.M., Borel, G., & Bussy, F. (2002). The organization of pre-Variscan basement  
1170 areas at the north-Gondwanan margin. *Int. J. Earth Sci.*, 91, 35-52.
- 1171 von Raumer, J.F., & Stampfli, G.M. (2008). The birth of the Rheic Ocean - Early Palaeozoic subsidence  
1172 patterns and tectonic plate scenarios. *Tectonophysics*, 461, 9-20.
- 1173 von Raumer, J.F., Bussy, F., Schaltegger, U., Schulz, B., & Stampfli, G.M. (2013). Pre- Mesozoic Alpine  
1174 basements -Their place in the European Paleozoic framework. *Geol. Soc. Am. Bull.*, 125, 89-108.
- 1175 von Riet, R. (1984). Intrusiva und Extrusiva der Bernina-Decke zwischen Morteratsch und Berninapass  
1176 (Graubünden). *Schweiz. Miner. Petrogr.*, 64, 83-109.
- 1177 Whalen, J.B., Currie, K.L., & Chappell, B.W. (1987). A-type granites geochemical characteristics,  
1178 discrimination and petrogenesis. *Contrib. Mineral. Petr.*, 95, 407-419.
- 1179 Williams, I.S. (1998). U-Th-Pb geochronology by ion microprobe. *Rev. Econ. Geol.*, 7, 1-35.
- 1180 Wilson, M. (1989). *Igneous Petrogenesis*. Unwin Hyman, London.
- 1181 Wilson, M., Neumann, E-R., Davies, G.R., Timmerman, M.J., Heeremans, M., & Larsen, B.T. (2004).  
1182 Permo-Carboniferous magmatism and rifting in Europe: introduction. In M. Wilson, E-R Neumann,  
1183 G.R. Davies, M.J. Timmerman, M. Heeremans, B.T. Larsen (Eds.), *Permo-Carboniferous Magmatism  
1184 and Rifting in Europe* (Vol. 223, pp. 1-10). Sp. Publ., Geol. Soc. London.
- 1185 Žák, J., Kratinova, Z., Trubac, J., Janousek, V., Slama, J., & Mrlna, J. (2011). Structure, emplacement, and  
1186 tectonic setting of Late Devonian granitoids plutons in the Tepla-Barrandian unit, Bohemian Massif. *Int.  
1187 J. Earth Sci.*, 100, 1477-1495.
- 1188 Žák, J., Verner, K., Janousek, V., Holub, F. V., Kachlik, V., Finge, F., Hajna, J., Tomek, F., Vondrovic, L.,  
1189 & Trubac, J. (2014). A plate-kinematic model for the assembly of the Bohemian Massif constrained by  
1190 structural relationships around granitoid plutons. In by K. Schulmann, J. R. Martínez Catalán, J. M.  
1191 Lardeaux, V. Janousek, G. Oggiano (Eds.), *The Variscan orogeny: extent, timescale and the formation  
1192 of the European crust* (Vol. 405, pp. 169-196). Sp. Publ., Geol. Soc. London.
- 1193
- 1194

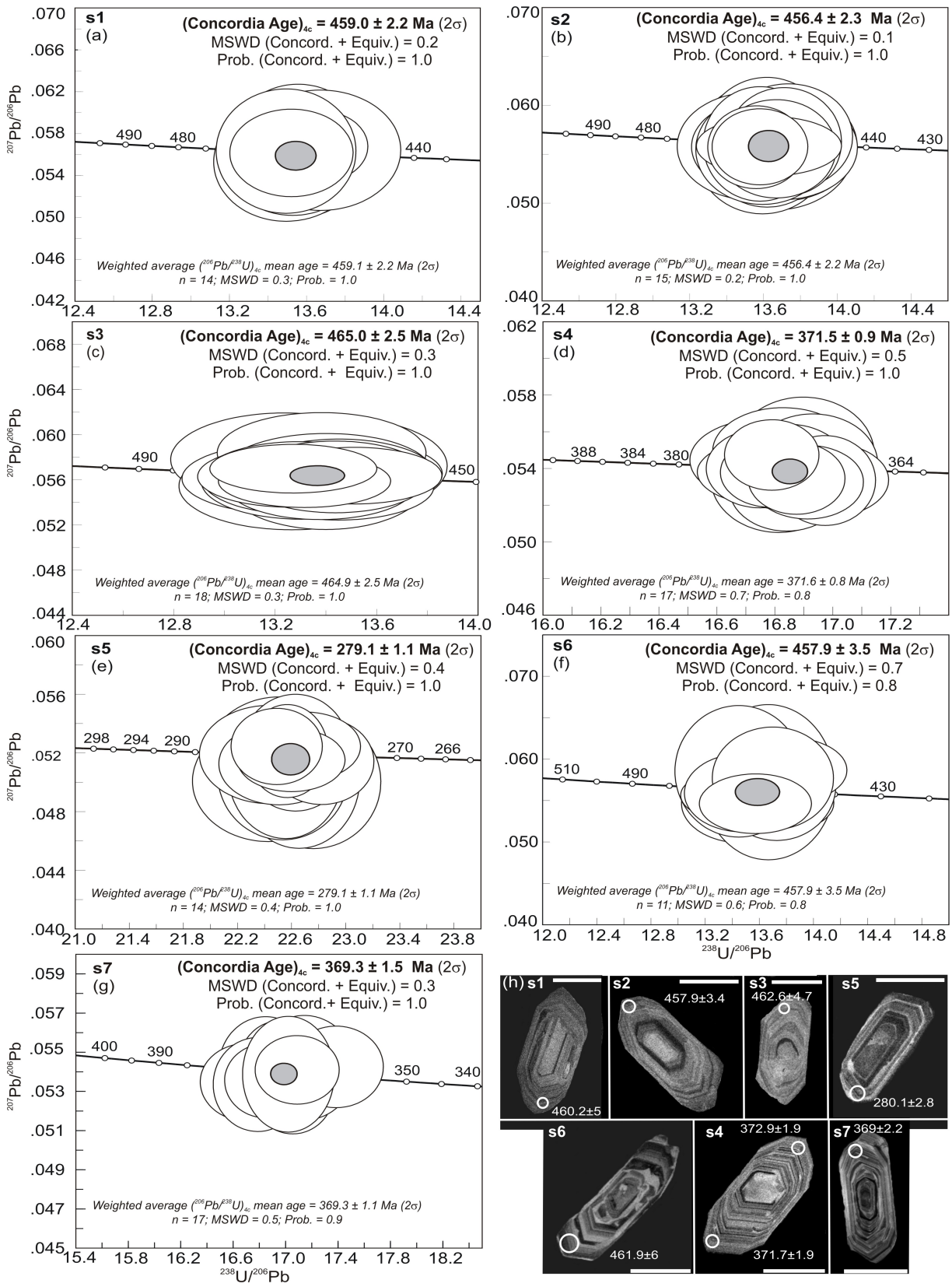


1197 **Figure 1.** (a) Tectonic sketch map of the Western and Central Alps; (b) 3D model of the Western  
 1198 Alps along cross section X-X' (after Malusà et al., 2015). Black stars indicate the location of dated  
 1199 samples (s1 to s7). Acronyms: AA, Aar; AR, Argentera; BE, Belledonne; DM, Dora-Maira; GF,  
 1200 Giudicarie Fault; GO, Gotthard; GP, Gran Paradiso HE, Helvetic; IF, Insubric Fault; IV, Ivrea-  
 1201 Verbano; LB, Ligurian Briançonnais; MB, Mont Blanc; MR, Monte Rosa; PE, Pelvoux; PFT,  
 1202 Penninic Frontal Thrust; SL, Sesia-Lanzo; SV, Sestri-Voltaggio Fault; VO, Voltri; VV,  
 1203 Villalvernia-Varzi Fault.

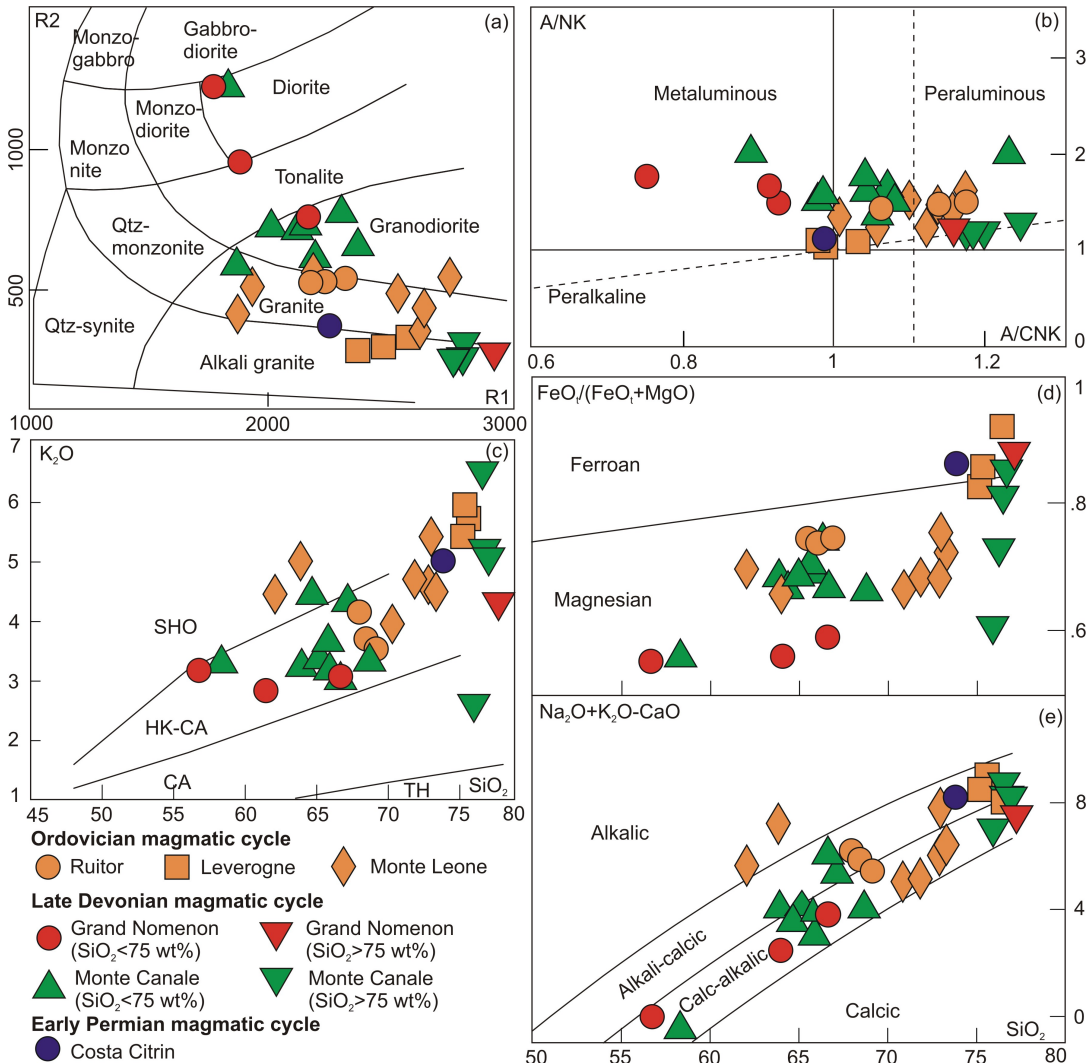
1205



1206 **Figure 2.** Tectonic map of the Grand St Bernard – Briançonnais nappe system and surrounding units in  
 1207 the Aosta Valley (modified after Polino et al., 2015; post-metamorphic faults after Malusà et al., 2009).  
 1208

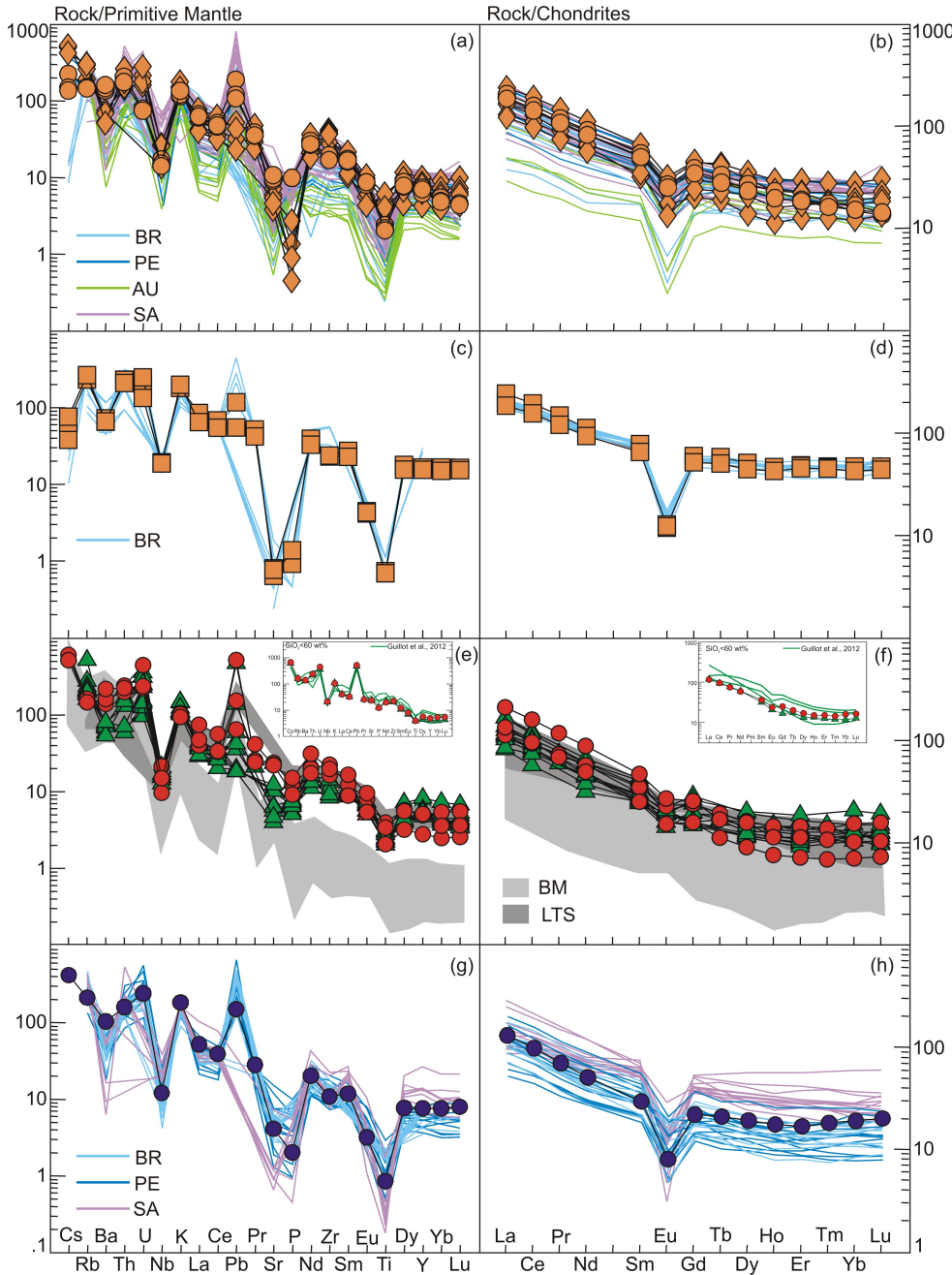


1210 **Figure 3.** (a-g) Tera-Wasserburg Concordia diagrams (Tera & Wasserburg, 1972) for samples s1 to  
1211 s5 from the Grand St Bernard – Briançonnais nappe system, s6 from the Monte Leone nappe, and  
1212 s7 from the Gneiss del Monte Canale unit. Dark gray ellipses represent Concordia ages; subscript  
1213 4c indicates  $^{204}\text{Pb}$  common lead correction. Individual error ellipses are given at 2-sigma level; n:  
1214 number of analyses; Equiv.: Equivalence; MSWD: Mean Square of Weighted Deviates; Prob.:  
1215 Probability of fit. (h) CL images of representative zircon grains. Circles indicate locations for U-Pb  
1216 dating by SHRIMP; numbers denote  $^{206}\text{Pb}/^{238}\text{U}$  ages with 1-sigma error; white bars are 100  $\mu\text{m}$ .  
1217



1219 **Figure 4.** Classification of analyzed samples based on geochemical data. a) R1-R2 classification  
1220 diagram of the De la Roche et al. (1980). R1 (millications)= $4\text{Si}-11(\text{Na}+\text{K})-2(\text{Fe}+\text{Ti})$  and R2  
1221 (millications)= $6\text{Ca}+2\text{Mg}+\text{Al}$ ; b) A/NK [molar ratio  $\text{Al}_2\text{O}_3/(\text{Na}_2\text{O}+\text{K}_2\text{O})$ ] vs A/CNK [molar ratio  
1222  $\text{Al}_2\text{O}_3/(\text{CaO}+\text{Na}_2\text{O}+\text{K}_2\text{O})$ ]; c)  $\text{K}_2\text{O}$  (wt%) vs  $\text{SiO}_2$  (wt%) classification diagram of Peccerillo &  
1223 Taylor, 1976. TH: Tholeiitic series, CA: calc-alkaline series, HK-CA: high-K calc-alkaline series,  
1224 SHO: shoshonite; d)  $\text{FeO}_t/(\text{FeO}_t+\text{MgO})$  vs  $\text{SiO}_2$  (wt%) discrimination diagram of Frost et al.  
1225 (2001); e)  $\text{K}_2\text{O}+\text{Na}_2\text{O}-\text{CaO}$  (wt%) vs  $\text{SiO}_2$  (wt%) discrimination diagram of Frost et al. (2001).

1226

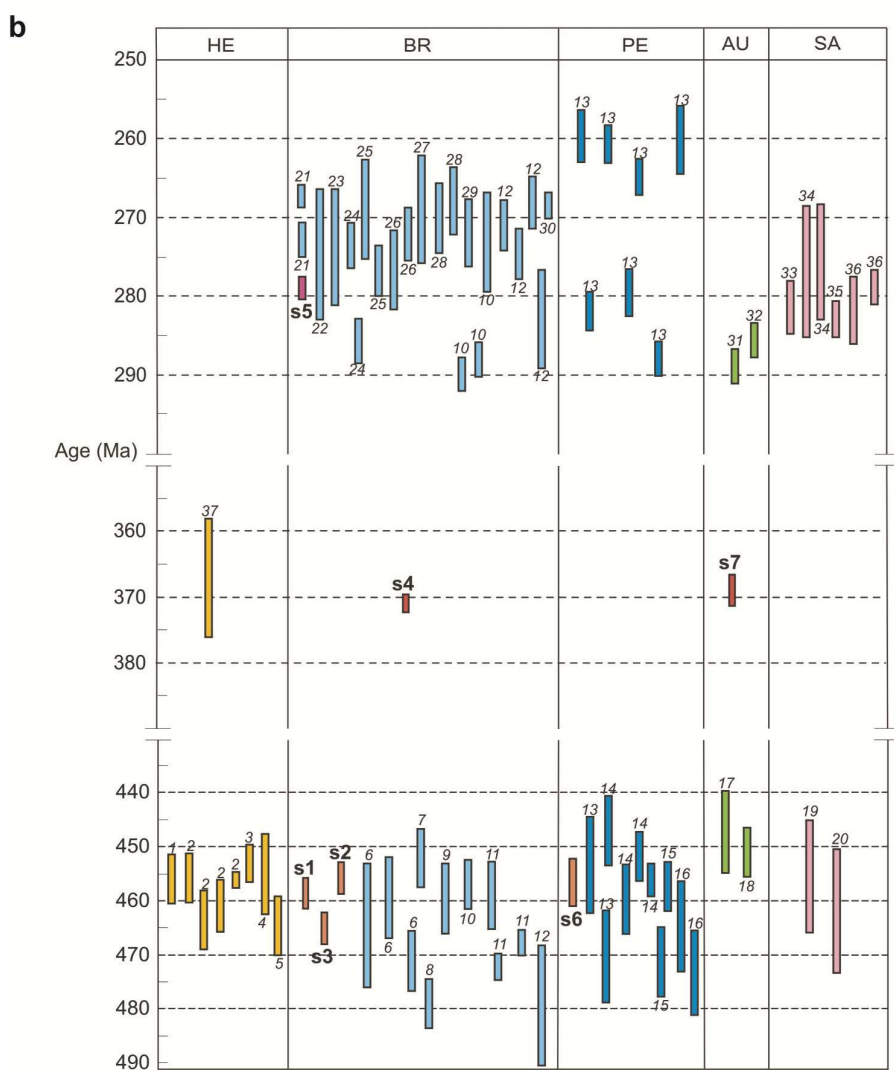
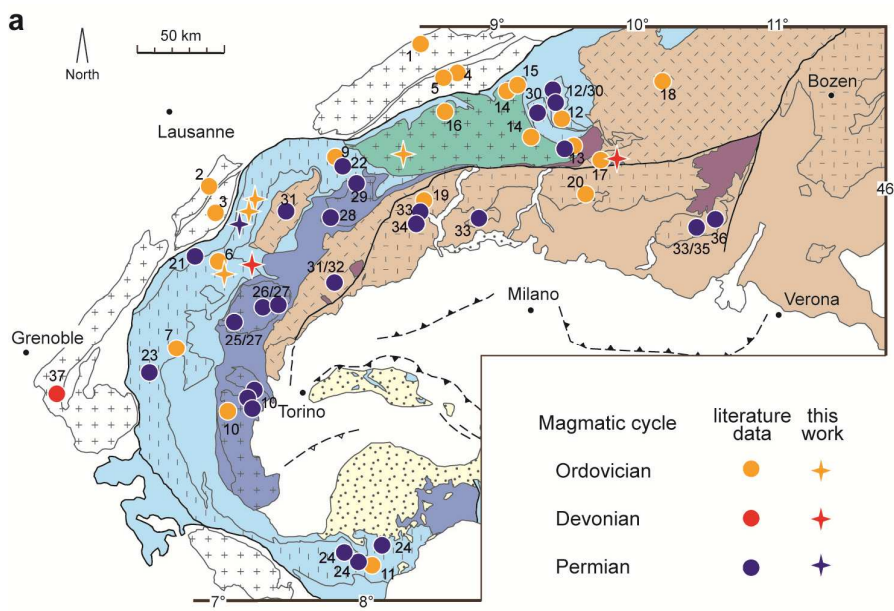


1227

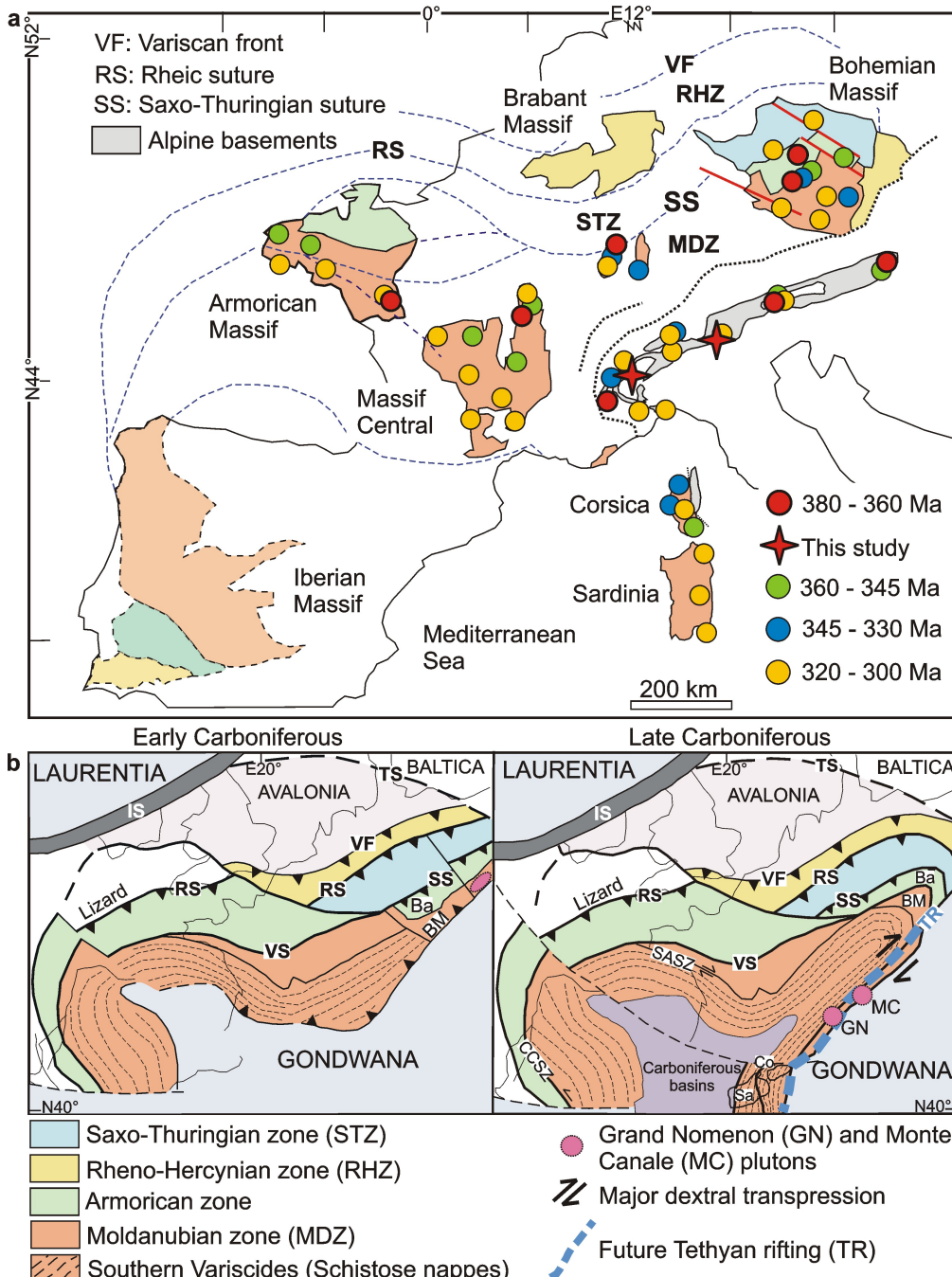
1228 **Figure 5.** (a-c-e-g) Primitive mantle (PM) normalized trace element (Sun & McDonough, 1989)  
 1229 and (b-d-f-h) Chondrite-normalized rare earth (REE) element (Sun & McDonough, 1989) diagrams  
 1230 for analyzed samples (symbols as in Figure 4). In (a), (b), (c) and (d), Middle to Upper Ordovician  
 1231 orthogneisses from Briançonnais (BR), other Penninic (PE), Austroalpine (AU) and Southalpine  
 1232 (SA) basements are plotted for comparison. Data sources. BR: Guillot et al. (2002), Beucler et al.

1233 (2000), Cosma (1999), Bertrand et al. (1998), Bussy & Cadoppi (1996), Guillot et al. (1993) and  
1234 Thélin et al. (1993); PE: Caravagna-Sani et al. (2014) and Bussien et al. (2011); AU: Boriani et al.  
1235 (2012a) and Schaltegger et al. (1997); SA: Pezzotta and Pinarelli (1994). In (e) and (f), fields of  
1236 Upper Devonian granitoids from Bohemian Massif (BM) and French Limousin Tonalite Suite  
1237 (LTS) are plotted for comparison. Data sources. BM: Žák et al. (2011, 2014) and Janousek et al.  
1238 (2000, 2004); LTS: Shaw et al. (1993). Inset: (e) PM and (f) REE normalized multi-element  
1239 variation diagrams for samples with  $\text{SiO}_2 < 60$  wt% compared with those of Guillot et al. (2012). In  
1240 (g) and (h), Lower Permian magmatic products from Briançonnais (BR), other Penninic (PE) and  
1241 Southalpine (SA) domains are plotted for comparison. Data sources. BR: Pawlig & Baumgartner  
1242 (2001), Bertrand et al. (1998), Marquer et al. (1998) and Bussy and Cadoppi (1996); PE:  
1243 Caravagna-Sani et al. (2014) and Galli et al. (2012); SA: Pinarelli et al. (1988) and Bakos et al.  
1244 (1990).

1245



1247 **Figure 6.** Age map (a) and table distribution (b) of the Middle to Upper Ordovician, Upper  
1248 Devonian and Lower Permian granitic protoliths in the Western and Central Alps to the West of  
1249 the Giudicarie Fault (numbers 1 to 37 indicate literature data): 1) Schaltegger et al. (2003), 2)  
1250 Bussy et al. (2011), 3) Bussy & von Raumer (1994), 4) Schaltegger (1994), 5) Oberli et al. (1994),  
1251 6) Guillot et al. (2002), 7) Bertrand et al. (2000a), 8) Bertrand & Leterrier (1997), 9) Genier et al.  
1252 (2008), 10) Bussy & Cadoppi (1996), 11) Gaggero et al. (2004), 12) Scheiber et al. (2013), 13)  
1253 Galli et al. (2012), 14) Caravagna-Sani et al. (2014), 15) Liati et al. (2009), 16) Bussien et al.  
1254 (2011), 17) Boriani et al. (2012a), 18) Flisch (1987), 19) Pezzotta & Pinarelli (1994), 20) Bergomi  
1255 et al. (2004), 21) Beltrando et al., (2007), 22) Bussy et al. (1996b), 23) Derron et al. (2006), 24)  
1256 Dallagiovanna et al. (2009), 25) Bertrand et al. (2000a), 26) Bertrand et al. (2005), 27) Ring et al.  
1257 (2005), 28) Pawlig & Baumgartner (2001), 29) Liati et al. (2001), 30) Marquer et al. (1998), 31)  
1258 Bussy et al. (1998), 32) Paquette et al. (1989), 33) Schaltegger & Brack (2007), 34) Pinarelli et al.  
1259 (1988), 35) Schaltegger & Brack (1999), 36) Gretter et al. (2013), 37) cited in Guillot and Ménot  
1260 (2009). Emplacement ages of basic protoliths are cited in the text. HE: Helvetic; BR:  
1261 Briançonnais; PE: other Penninic; AU: Austroalpine; SA: Southalpine.  
1262



1263

1264 **Figure 7.** a) Simplified sketch map of the European Variscides (modified after Faure et al., 2005;  
1265 Guillot & Ménot, 2009; Žák et al., 2014) showing basement distribution and representative Late  
1266 Devonian to Late Carboniferous magmatic pulses (based on this work and literature data from  
1267 Debon & Lemmet, 1999; Eichhorn et al., 2000; Faure et al., 2005; Guillot & Ménot, 2009;

1268 Neubauer et al., 2003; Rossi et al., 2009; Schaltegger, 2000; Tabaud et al., 2014; Žák et al., 2014);  
1269 b) Inferred position of the Grand Nomenon and Monte Canale plutons in the Variscan belt of  
1270 western Europe during the Early and Late Carboniferous (modified after Carosi et al., 2012;  
1271 Duchesne et al., 2013; Edel et al., 2013; Guillot & Ménot, 2009, Matte, 2001; Rossi et al., 2009).  
1272 Major dextral transpression at 320–300 Ma according to Rolland et al. (2009). Ba: Barradian unit;  
1273 BM: Bohemian Massif; CCSZ: Coimbra-Cordoba Shear Zone; Co: Corsica; IS: Iapetus suture; Sa:  
1274 Sardinia; SASZ: South Armorican Shear Zone; TS: Tornquist suture; VS: eo-Variscan suture.  
1275

1276 **SUPPORTING INFORMATION:**

1277 **Supplementary Table TS01:** SHRIMP U-Pb analyses

1278 **Supplementary Table TS02:** Whole rock compositions

1279 **Supplementary Table TS03:** Sample locations, petrography and geochronology

1280 **Supplementary Methods**